



This is a repository copy of *Seismic performance assessment of steel buildings equipped with a new semi-active displacement-dependent viscous damper*.

White Rose Research Online URL for this paper:

<https://eprints.whiterose.ac.uk/219076/>

Version: Published Version

---

**Article:**

Kiral, A. [orcid.org/0000-0002-4534-3686](https://orcid.org/0000-0002-4534-3686), Garcia, R. [orcid.org/0000-0002-6363-8859](https://orcid.org/0000-0002-6363-8859), Petkovski, M. [orcid.org/0000-0002-3788-0772](https://orcid.org/0000-0002-3788-0772) et al. (1 more author) (2024) Seismic performance assessment of steel buildings equipped with a new semi-active displacement-dependent viscous damper. *Journal of Earthquake and Tsunami*, 18 (06). ISSN 1793-4311

<https://doi.org/10.1142/s1793431124500222>

---

**Reuse**

This article is distributed under the terms of the Creative Commons Attribution (CC BY) licence. This licence allows you to distribute, remix, tweak, and build upon the work, even commercially, as long as you credit the authors for the original work. More information and the full terms of the licence here:

<https://creativecommons.org/licenses/>

**Takedown**

If you consider content in White Rose Research Online to be in breach of UK law, please notify us by emailing [eprints@whiterose.ac.uk](mailto:eprints@whiterose.ac.uk) including the URL of the record and the reason for the withdrawal request.



[eprints@whiterose.ac.uk](mailto:eprints@whiterose.ac.uk)  
<https://eprints.whiterose.ac.uk/>

## Seismic Performance Assessment of Steel Buildings Equipped with a New Semi-active Displacement-Dependent Viscous Damper

Adnan Kiral <sup>\*,¶</sup>, Reyes Garcia <sup>†,||</sup>, Mihail Petkovski <sup>‡,\*\*\*</sup>  
and Iman Hajirasouliha <sup>§,††</sup>

*\*Department of Civil Engineering  
Faculty of Engineering and Architecture  
Recep Tayyip Erdogan University  
Rize 53100, Turkey*

*†Civil Engineering Stream, School of Engineering  
The University of Warwick, Coventry, UK*

*‡The University of Sheffield, Sheffield, UK*

*§Department of Civil and Structural Engineering  
The University of Sheffield, Sheffield, UK  
¶[adnan.kiral@erdogan.edu.tr](mailto:adnan.kiral@erdogan.edu.tr)*

*||[Reyes.Garcia@warwick.ac.uk](mailto:Reyes.Garcia@warwick.ac.uk)*

*\*\*[mihailpetkovski@gmail.com](mailto:mihailpetkovski@gmail.com)*

*††[i.hajirasouliha@sheffield.ac.uk](mailto:i.hajirasouliha@sheffield.ac.uk)*

Received 27 March 2024

Revised 25 May 2024

Accepted 23 June 2024

Published 8 August 2024

This paper investigates numerically the seismic behavior of multi-degree-of-freedom (MDOF) systems with novel 2–4 direction and displacement-dependent (2–4DDD) and 2–4 Displacement-Velocity- (2–4DVD) Semi-Active (SA) controls. This study builds upon the novel SA 2–4DDD control system, in which the damper forces are controlled by inter-story drifts. For the first time, this paper investigates numerically the behavior of an MDOF system with 2–4DDD controls. A 3-story steel frame is modeled in OpenSees and then subjected to real earthquake records. The frame is modeled considering three control systems: (i) conventional passive nonlinear viscous dampers (NVDs), (ii) SA 2–4DDD dampers, and (iii) a new 2–4DVD SA damper. Parametric studies are conducted to determine the optimal parameters of 2–4DVD control in the designed frames. New design methodologies for MDOF systems with 2–4DVD and 2–4DDD controls are also proposed. The results are discussed in terms of inter-story drift, base shear force, acceleration, dissipated energy and required damper force. Results from Nonlinear Time History Analyses show that, compared to a frame with traditional NVDs, the inter-story drifts and base shear of the frame with 2–4DVD control are up to 72% and 32% lower,

<sup>¶</sup>Corresponding author.

This is an Open Access article published by World Scientific Publishing Company. It is distributed under the terms of the [Creative Commons Attribution 4.0 \(CC BY\) License](https://creativecommons.org/licenses/by/4.0/), which permits use, distribution and reproduction in any medium, provided the original work is properly cited.

respectively. 2–4DVD control also reduces damping forces and acceleration by up to 60% and 87%, respectively, compared to 2–4DDD control. It is also shown that the 2–4DDD control was not stable in high-frequency earthquake records. Conversely, the new 2–4DVD control leads to smoother damping force changes between quadrants for the case study investigated in this paper. This study contributes toward the development of new seismic retrofitting dampers for nonlinear MDOF systems.

*Keywords:* Seismic behavior; semi-active control; viscous dampers; steel frames; hysteretic response.

## 1. Introduction

In the last decades, structural control systems have become a popular alternative to reduce damage in buildings located in earthquake-prone regions [Etedali *et al.*, 2023; Hosseini Lavassani *et al.*, 2022; Meigooni and Tehranizadeh, 2022]. Whilst the initial cost of structural control systems can be relatively high compared to the total cost of the building, they are deemed as a viable option because they (i) increase significantly the energy dissipation capacity of buildings [Karami Mohammadi *et al.*, 2021], (ii) speed up construction as elements can be standardized and built off-site, and (iii) reduce the cost of eventual post-earthquake repairs in case buildings experience damage [Quintana and Petkovski, 2018]. Among the different structural control systems currently available, dampers are probably one of the most widely adopted devices. Different types of dampers exist for buildings. For example, Fluid Viscous Dampers (FVDs) dissipate energy that enters the building during an earthquake by compressing fluids stored in the damper. The main advantages of passive FVDs are that they do not need any external power source to operate, they have simple working mechanisms and they require little maintenance after installation [Symans and Constantinou, 1995]. Previous experimental and numerical studies [Abdulahadi *et al.*, 2020a,b; Akehashi and Takewaki, 2019; Aydin *et al.*, 2019; Chan and Quincy, 2022; Dall’Asta *et al.*, 2016; Domenico and Hajirasouliha, 2021; Dong *et al.*, 2016; Jiao *et al.*, 2018; Kiral and Gurbuz, 2024; Lin *et al.*, 2017; Riaz *et al.*, 2023] have proven that FVDs are effective at reducing structural damage by absorbing a significant portion of the input energy from an earthquake. Moreover, FVDs have been successfully used to reduce the seismic demands on structures. For example, Domenico and Hajirasouliha [2021] proved that the adoption of a Uniform Damage Distribution (UDD) concept for the design of FVDs reduced maximum plastic rotations in frames by 38%. Past research has also verified the effectiveness of nonlinear viscous dampers (NVDs) in controlling the response of structures. Lin and Chopra [2002] found that the use of NVDs on Single-Degree-of-Freedom (SDOF) systems reduced structural deformations by up to 60%. Riaz *et al.* [2023] showed that using NVDs in buildings reduced the inter-story drifts by approximately 31%. However, previous research has also shown that the use of viscous dampers as retrofitting devices can increase the base shear of buildings, especially in buildings experiencing nonlinear behavior [Domenico and Hajirasouliha, 2021; Hazaveh *et al.*,

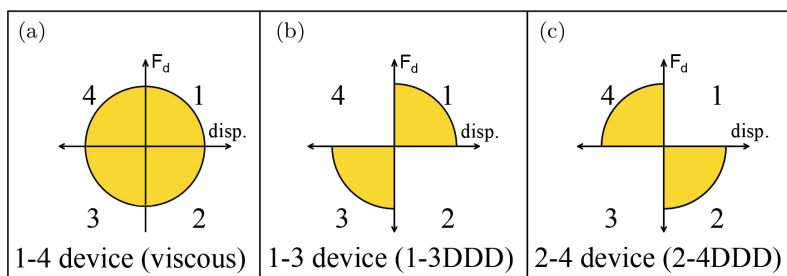


Fig. 1. Force–displacement hysteretic loops of (a) 1–4 conventional viscous device, (b) 1–3 devices (1–3DDD, quadrants 1 and 3 displacement–direction–dependent), and (c) 2–4 devices (2–4DDD).

2016]. Indeed, [Domenico and Hajirasouliha \[2021\]](#) found that the use of NVDs increased the total base shear of substandard moment-resisting steel frames by up to 15%. Such an increase in the frame’s base shear can hinder the use of viscous dampers in retrofitting applications due to the additional costs associated with the need to retrofit the building’s ground floor columns and foundations.

Conventional linear viscous dampers provide damping forces in all four quadrants of their force–displacement hysteretic loops, as shown schematically in Fig. 1(a) (1–4 devices). In large damping applications of linear frames and even in small damping applications of nonlinear frames, the viscous damper forces act in phase with the frame forces. Accordingly, an increase in the base shear of the system is inevitable while dampers are being used to reduce the frame’s displacements. The reshaped force–displacement loop of a viscous damper could be a solution to be out of phase with structural forces in low or high structural damping applications. A reshaped force–displacement hysteresis of the viscous damper could also be a cost-effective solution for seismic retrofitting of existing buildings, mainly because of the cost and challenges resulting from retrofitting the building’s ground floor columns and foundations.

Semi-active (SA) control systems operated by a small external power source were proposed by [Symans and Constantinou \[1995\]](#). A main advantage of SA control devices is that they can operate as passive devices even if a power cut occurs. Moreover, SA devices do not add energy to the system. Instead, they store/absorb the vibration energy input from earthquakes. Therefore, such devices do not destabilize structural frames like active systems [[Chase et al., 2006](#); [Hazaveh et al., 2017b](#)]. SA systems only control the behavior of a structure by changing its damping [[Fukuda and Kurino, 2019](#); [Hazaveh et al., 2017b](#); [Kurino et al., 2003](#)] or stiffness [[Mulligan et al., 2010](#)], whereas other properties remain constant.

The behavior of SA viscous dampers is heavily dominated by their force–displacement hysteresis loops. Most SA viscous dampers proposed in the current literature [[Dan et al., 2015](#); [Ho et al., 2018](#); [Symans and Constantinou, 1995](#)] provide damping forces in all four quadrants of their force–displacement loops. However, [Hazaveh et al. \[2017b\]](#) proposed to “reshape” the force–displacement loops of viscous dampers to enhance their effectiveness. [Hazaveh et al. \[2017b\]](#) investigated a linear SDOF steel frame with SA control and damper motion resisted in either (i) all four

quadrants (1–4 conventional viscous dampers, Fig. 1(a)), (ii) motion away from equilibrium (1–3 damper, Fig. 1(b)), and (iii) motion toward equilibrium (2–4 damper, Fig. 1(c)). They found that reshaped viscous dampers with a 2–4 control loop (2–4DDD; DDD = direction and displacement-dependent, Fig. 1(c)) did not increase the base shear of buildings because the damper forces and column forces are completely out of phase. However, the 1–3 control tended to increase the base shear of the frame in the case of large damping because the damper forces (1–3 control) and column forces are partially in phase with each other. They also found that the 2–4 control reduced the average values of maximum acceleration, total base shear, and maximum displacement by 10–40% over all periods (up to 5.0 s) when compared to the uncontrolled frame. Control loops 1–3 and 1–4 reduced the maximum displacement by similar magnitudes (or even more) but at the expense of increasing the frame's base shear. While 2–4 dampers (or 2–4DDD) have proven more advantageous than other devices (1–3 and 1–4) to control damage in structures, to date no research has investigated their use in multi-degree-of-freedom (MDOF) systems. As a result, research is necessary to provide further insight into the effectiveness of 2–4DDD devices in controlling the response of multi-story buildings.

For the first time, this paper examines numerically the seismic behavior of an MDOF system with a 2–4DDD control that incorporates a sudden opening and closing algorithm between quadrants of a viscous damper. In the presence of unstable behavior of 2–4DDD over a wide range of seismic frequencies, this study proposes a novel control device called 2–4DVD, which facilitates smooth changes in damping force between quadrants. To achieve this, a nonlinear 3-story frame building is modeled in OpenSees software and subjected to a set of four real PEER seismic records. The frame is modeled with three different controls: (i) passive NVDs (with  $\alpha = 0.3$ ) which serve as a comparative benchmark, (ii) 2–4DDD dampers, and (iii) a new SA 2–4DVD damper (2–4 Displacement-Velocity-Dependent) proposed in this study. Parametric studies are conducted to determine the optimum parameters of 2–4DDD and 2–4DVD controls in the frames. A design methodology for the new 2–4DVD control is also proposed. The outcomes of this study contribute toward the development of innovative dampers suitable for use in the seismic retrofitting of substandard buildings.

## 2. Numerical Study

### 2.1. Design and analysis of steel frames

The MDOF system considered in this study is a 3-story steel moment-resisting frame (MRF) with a total height of 9.6 m and a total width of 15.0 m (see Fig. 2(a)). The 2D bare frame is designed to withstand horizontal loads and gravity loads, with the former being calculated using the design spectrum in CEN Eurocode 8 [2004]. The design considers that the bare frame is in a low seismic activity area with a Peak Ground Acceleration  $PGA = 0.18 g$ . A ground type C (shear wave velocity

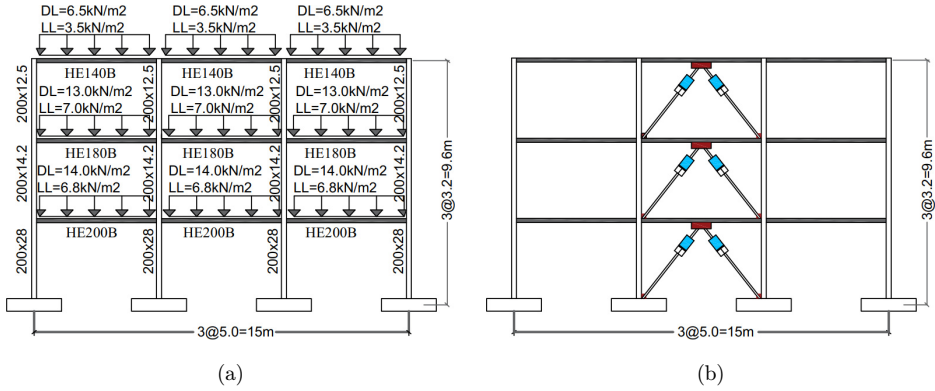


Fig. 2. (a) Loads and element sections in bare steel frame (no viscous dampers), and (b) counterpart steel frame with viscous dampers.

$V_s = 180\text{--}360\text{ m/s}$ ) and a behavior factor  $q = 6.5$  are assumed for the design. The corresponding dead (DL) and live loads (LL) are assumed to be  $14.0\text{ kN/m}^2$  and  $6.8\text{ kN/m}^2$  for the first story,  $13.0\text{ kN/m}^2$  and  $7.0\text{ kN/m}^2$  for the second story, and  $6.5\text{ kN/m}^2$  and  $3.5\text{ kN/m}^2$  for the third story, as shown in Fig. 2(a).

It is assumed that the first-story columns are fixed to the ground, and that beams and columns are rigidly connected. As the building is designed to be highly ductile under strong earthquake shaking, the nonlinear contribution of the beams to the structural behavior is considered by not assigning rigid diaphragms to the floors in the models. It is also assumed that beams and columns are made of steels S275 and S355, with respective nominal yield strengths of 275 MPa and 355 MPa. A strain-hardening ratio of 1% is chosen for simplicity. Nonlinear time-history analyses (NTHAs) in OpenSees software are conducted to design the frame, as per CEN Eurocode 8 §4.2.3 [2004]. Moreover, a strong column-weak beam design philosophy was adopted according to Eurocode 8, which resulted in the cross-sections presented in Fig. 2(a). The steel sections resulting from the design of the bare frame is shown in Fig. 2(a). Wide flange HEB profiles are used for beams (e.g. HEB200B has a cross-section of 200 mm width  $\times$  200 mm depth), while square hollow sections are used for columns (e.g. 200  $\times$  28 is a square section with a side of 200 mm and a thickness of 28 mm). According to test results by Akcelyan *et al.* [2016] and numerical analyses of Huang [2009], the stiffness of braces (supporting braces) connected to viscous dampers can change the performance of the dampers. To avoid such issues in the analysis, this study adopts a realistic value of brace stiffness (see Sec. 2.3) given by Taylor Device Inc. [2020]. The fundamental period of the 3-story steel bare frame is calculated as 0.93 s. Note that since a viscous damper response is velocity-dependent (as shown later in Eq. (1)), the use of dampers on the steel frame is not expected to change such a period.

After the design, the model of the bare frame was modified to account for the control devices. Three case study frames with different viscous dampers in a

Chevron brace configuration are considered, according to the geometry shown in Fig. 2(b):

- a frame with a NVD control,
- a frame with a 2-4DDD damper control, and
- a frame with a 2-4DVD control.

The connection between the dampers and the frame is modeled as a joint (“nodes”) in OpenSees. The dampers of the three steel frames adopt the modeling approaches described later in Sec. 0. The nonlinear dynamic response of the three case study frames is carried out using OpenSees [McKenna et al., 2006]. The beams and columns (class 1 cross-sections) are modelled using beam-column elements with force-based distributed plasticity (type “nonlinearBeamColumn”). Five Gauss–Lobatto integration points were used along the elements’ length. Whilst the adoption of displacement-based controls in OpenSees would be computationally less demanding than the use of force-based elements, it would require a mesh refinement and sensitivity analysis to improve the accuracy of the local solutions. Accordingly, adopting force-based elements is advantageous, as they only need a larger number of integration points in each element to improve accuracy. A bilinear steel (*Steel01*) material is adopted in the modeling of the elements. For computational efficiency, the cross-sections of beams (with wide flanges) and columns (with hollow square tubes) are discretized using 40 and 52 fibers, respectively, according to the recommendations by Kostic and Filippou [2012]. A Rayleigh damping ratio of 2% is used to model inherent damping corresponding to the first mode and to the mode associated with cumulative mass participation exceeding 95%. Likewise, a Newmark constant-average acceleration scheme is used to integrate the equations of motion over time. Geometric nonlinearities (e.g. P-Delta transformations) are also considered in the modeling. The three case study frames were subsequently subjected to a set of seismic records, which are described in the following section.

## 2.2. Seismic records

In this study, four real seismic records with different predominant frequency ranges are selected from the PEER [2023] ground motion database. Table 1 lists the main characteristics of the records, whereas Fig. 3 shows their corresponding response spectra.

Table 1. Characteristics of selected seismic records used in this study.

Earthquake	$M_w$	Abbreviation	Station ID/Component	PGA (g)
1992 Cape Mendocino	6.9	CAP	CAPEMEND/PET000	0.590
1994 Northridge-01	6.69	PAR	PARDEE/PAR-L	0.558
2007 Chuetsu-oki, Japan	6.8	CHU	Kashiwazaki, NPP/SG01EW	0.444
1995 Kobe	6.9	KOBE	Takatori/TAK090	0.616

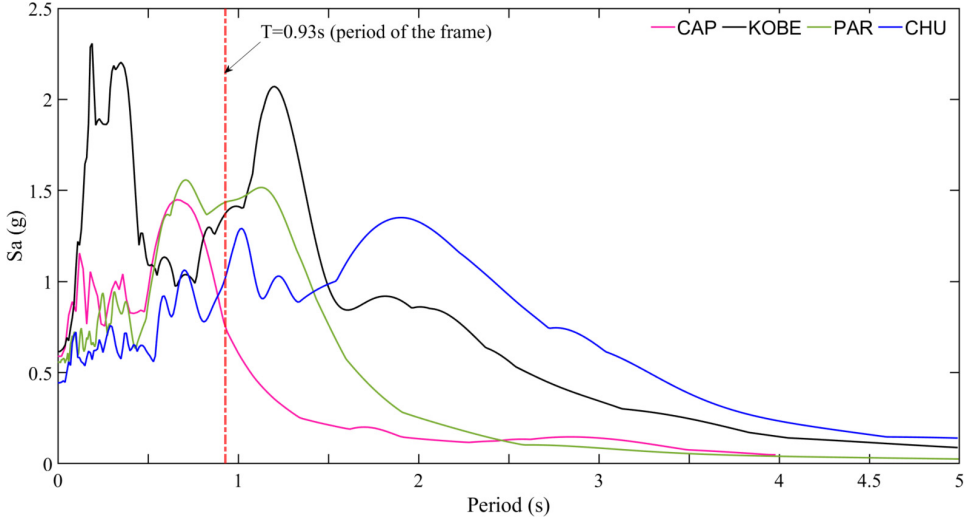


Fig. 3. Response spectra of selected seismic records.

It is shown that the selected records have PGAs well above the PGA used to design the steel frame ( $PGA = 0.18\text{ g}$ ), and therefore the frames are expected to be subject to large seismic demands. Figure 3 also shows the fundamental period of the 3-story steel frame. As it will be shown in Sec. 3, the 2-4DDD control is unstable under some of the seismic records, which makes direct comparisons between the three types of controls (NVD, 2-4DDD and 2-4DVD) difficult as convergence issues occurred during the analyses in OpenSees. Accordingly, this study considers only four seismic records for which no convergence issues and full results were obtained. Future research should investigate the adoption of other earthquake records and/or a design response spectrum as input in the nonlinear dynamic analyses.

### 2.3. Modeling of nonlinear viscous damper

The constitutive behavior of a fluid viscous damper (Fig. 4) can be modeled using a Maxwell stiffness ( $K_d^*$ ) and a dashpot with a fractional force-velocity relationship, according to Eq. (1) [Symans and Constantinou, 1995] and to the model shown in Fig. 4(a):

$$F_d = C_d |\dot{\delta}_d|^\alpha \text{sgn}(\dot{\delta}_d), \tag{1}$$

where  $F_d$  is the damper force;  $C_d$  is the damping coefficient;  $\dot{\delta}_d = \dot{\delta} \times \cos \theta$  is the relative velocity (i.e. inter-story velocity in damper, Fig. 4(a), between the two terminals of the device projected along the damper's axis;  $\alpha$  is the power-law non-linearity of the damper; and  $\text{sgn}(\cdot)$  is the sign function returning either a + or - value.

In this study, the inter-story velocity is multiplied by  $\cos \theta$ , where  $\theta = \arctan(2H/L)$  is the angle of the brace with respect to the horizontal axis, as defined by the geometry shown in Fig. 4(a). The hydraulic circuit used in the damper



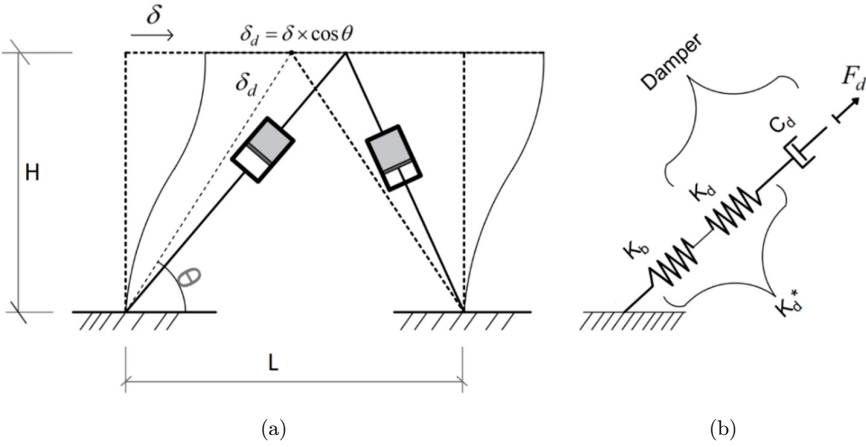


Fig. 4. (a) Schematic view of Maxwell model of NVD, and (b) damper model ( $K_b$  = brace stiffness;  $K_d^*$  = axial stiffness of damper;  $K_d^* = K_b + C_d$ ).

determines the magnitude of the velocity exponent  $\alpha$ . Past studies have reported that  $\alpha$  ranges between 0.2 and 1.0 for devices available in the market [Taylor Devices Inc., 2020]. Altieri et al. [2018] proved that the use of  $\alpha = 0.3$  in the analysis reduced the required damping forces by 30% compared to the use of  $\alpha = 1$ , while achieving the same drifts. Therefore, a velocity exponent  $\alpha = 0.3$  is adopted for modeling of nonlinear viscous damper (NVD) modeled in OpenSees.

NVDs are modeled in OpenSees using “twoNodeLink” elements with “ViscousDamper” materials [Akcelyan et al., 2016]. OpenSees adopts a Maxwell model that combines linear springs (\$K) and dashpots with a damping coefficient  $C_d$  and a velocity exponent  $a$ . The parameter \$K (or  $K_d^*$  in Fig. 4(b)) of all viscous dampers in the frame is  $K_d^*(\$K) = 3283.63 \text{ kN/cm}$ , according to recommendations by Taylor Devices Inc. [2020]. The element recorder “localForce” in the “twoNodeLink” elements is used to obtain the damper forces in OpenSees software. Damper limit states (typically associated with the maximum stroke limit of a piston during severe earthquakes [Miyamoto et al., 2010]) are ignored in the analysis because commercial dampers can have long strokes up to 900 mm [Taylor Devices Inc., 2020].

#### 2.4. Semi-active 2-4DDD control damper

Conventional viscous dampers (CVDs) resist forces in all four quadrants of the force-displacement hysteresis loop. CVDs reduce structural displacement demands via additional damping without increasing the base shear of frames. However, in nonlinear frames or frames with high levels of additional damping, they can easily increase the total base shear demand and this is an undesired effect. To bypass this drawback, a novel 2-4DDD control [Hazaveh et al., 2017b] proved effective at reducing displacements without increasing base shear. The 2-4DDD control removes the damping forces in quadrants 1 and 3 of the damper force-displacement hysteresis

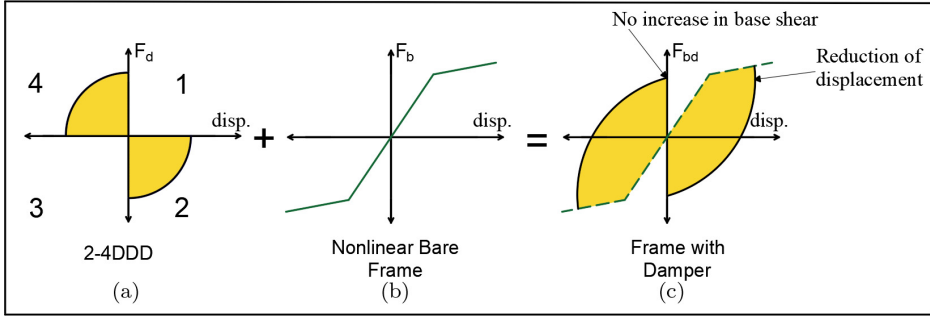


Fig. 5. Schematic representation of a 2-4DDD control.  $F_d$  = damper force.  $F_b$  = base shear for bare frame (without damper).  $F_{bd}$  = total base shear for damped structure.

loops (see Fig. 5(a)). The new reshaped force–displacement loop (Fig. 5(a)) is fully out of phase with frame forces, as shown in Figs. 5(b) and 5(c). To achieve the new loop, Hazaveh *et al.* [2017b] proposed Eq. (2) for the control of a viscous damper hysteresis loop. To model this type of control in OpenSees, an adhoc “for loop” command is written in the software. This “loop” checks Eq. (2) and decides if a force is needed in the damper. Based on this, the viscous damper coefficient is determined. After a full earthquake record simulation, an external subroutine written in MATLAB<sup>®</sup> environment [MATLAB, 2018] checks (or updates) the control parameters (Steps 3 and 5 in Fig. 6) before the next iteration (i.e. a full NTHA under the same earthquake records). The total base shear, which is needed in Steps 3 and 5 of Fig. 6, is also obtained in the software after performing a full NTHA.

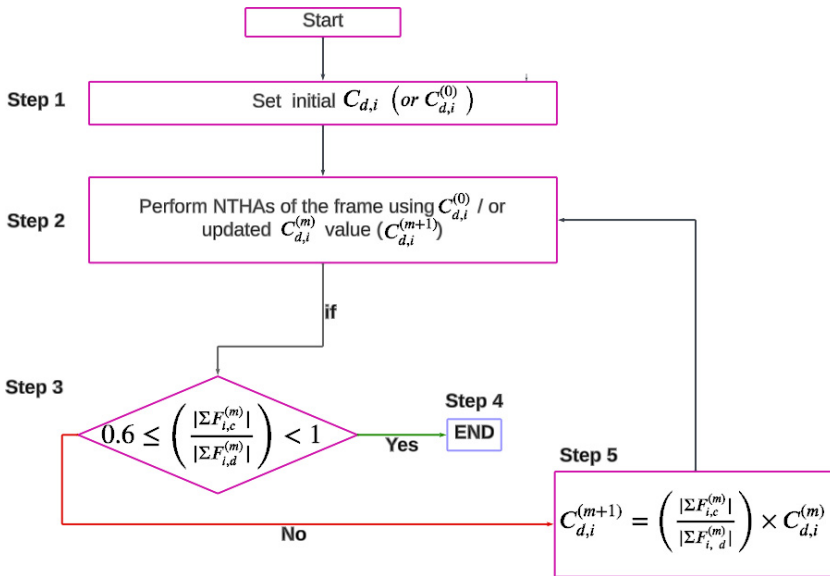


Fig. 6. Flowchart of proposed design methodology for 2-4DDD control.

It is assumed here that, since the velocity and displacement change over time, the orifices of the devices would open or close to produce damping in the desired quadrant. Accordingly:

$$2 - 4DDD \text{ control} \begin{cases} \text{if } \text{sgn}(\delta_{d,i}) \neq \text{sgn}(\dot{\delta}_{d,i}), & F_d = C_{d,i} \times \dot{\delta}_{d,i}, \\ \text{if } \text{sgn}(\delta_{d,i}) = \text{sgn}(\dot{\delta}_{d,i}), & F_{d,i} \approx 0, \end{cases} \quad (2)$$

where all variables are as defined before.

The flowchart in Fig. 6 proposes an iterative design methodology to calculate the damping coefficient of 2–4DDD control in a frame. Note that the methodology has to be applied to each story individually, according to the definition of  $\dot{\delta}_{d,i}$  in Eq. (2) (referring to local inter-story velocity in the damper at the  $i$ th story). The Steps of the design methodology can be summarized as follows:

**Step 1.** Choose an initial arbitrary damping coefficient  $C_{d,i}$  ( $C_{d,i}^{(0)}$ ) to input in Eq. (2). This initial  $C_{d,i}$  is updated using Eq. (4) at the end of each iteration (i.e. at the end of each NTHA analysis). Therefore, the initial value of  $C_{d,i}$  is not critical in the design.

**Step 2.** Perform a NTHA of the frame using  $C_{d,i}^{(0)}$  or updated  $C_{d,i}^{(m)}$  value ( $C_{d,i}^{(m+1)}$ ) under an earthquake record.

**Step 3.** Check if the condition defined in Eq. (3) is met:

$$0.6 \leq \left( \frac{\left| \sum F_{i,c}^{(m)} \right|}{\left| \sum F_{i,d}^{(m)} \right|} \right) < 1.0, \quad (3)$$

where  $\sum F_{1,d}^{(m)}$  is the total peak global damper forces (considering all columns) of the story  $i$  at iteration  $m$ ; and  $\sum F_{1,c}^{(m)}$  is the total peak force of all four columns in story  $i$  at iteration  $m$ . Note that the limits of 0.6 and 1.0 in Eq. (3) are set based on results from this study and could be slightly different for other case study structures. The convergence of Eq. (3) is generally achieved after a few iterations (usually fewer than 20), depending on the earthquake applied in the analysis.

**Step 4.** If the condition in Eq. (3) is met, end the simulation.

**Step 5.** If the condition in Eq. (3) is not met, then update the value of the parameter  $C_{d,i}^{(0)}$  or  $C_{d,i}^{(m)}$  based on the recurrence relationship in Eq. (4). Then repeat the process from Step 2 until the condition in Eq. (3) is met.

$$C_{d,i}^{(m+1)} = \left( \frac{\left| \sum F_{i,c}^{(m)} \right|}{\left| \sum F_{i,d}^{(m)} \right|} \right) \times C_{d,i}^{(m)}, \quad (4)$$

where  $C_{d,i}^{(m)}$  is the damping coefficient of the story  $i$  at iteration  $m$ ; and the rest of the variables are as defined before.

2.5. Semiactive 2-4DVD control damper

As it will be shown later, the 2-4DDD control can cause unstable damper loops under high-frequency ground excitations. Therefore, a new 2-4DVD control is proposed in this study as shown in Fig. 7(a). The control has closed orifices in quadrants 2 and 4 from the peak dashpot displacement back toward zero displacements, and partially locked orifices in quadrants 1 and 3. This leads to full damping resistance in quadrants 2 and 4 (Eq. (5a)), and to partial damping resistance in quadrants 1 and 3 (see also Eq. (5b)). This control is similar to 2-4DDD control, but it offers more stable damping force changes between quadrants by providing some forces in quadrants 1 and 3 (Figs. 7(b) and 7(c)). The modeling, parameters optimization procedure of the control in the software are the same as those of the 2-4DDD control (see Sec. 2.4), but the main difference is the governing equations (see Eqs. (2) and (5)).

The proposed algorithm of 2-4DVD control is defined by Eqs. (5a) and (5b):

$$\begin{cases}
 \text{if } \text{sgn}(\delta_{d,i}) \neq \text{sgn}(\dot{\delta}_{d,i}), F_{d,i}^j = C_{d,i,2-4}^j \times \dot{\delta}_{d,i}^j \\
 = \begin{cases} C_{d,i,2-4}^j = \frac{A_{d,i,2-4}^j \times C_{d,in}}{F_{d,i}^{j-1}}, \\ A_{d,i,2-4}^j = \frac{K_i}{1 + e^{(0.01 \times |\dot{\delta}_{d,i}^{j-1}| - 10)}}, \\ \frac{A_{d,i,2-4}^j}{F_{d,i}^{j-1}} \leq G, \end{cases} \\
 \text{if } \text{sgn}(\delta_{d,i}) = \text{sgn}(\dot{\delta}_{d,i}), F_{d,i}^j = C_{d,i,1-3}^j \times \dot{\delta}_{d,i}^j \\
 = \begin{cases} C_{d,i,1-3}^j = \frac{A_{d,i,1-3}^j \times C_{d,in}}{F_{d,i}^{j-1}}, \\ A_{d,i,1-3}^j = \frac{K_i}{1 + e^{(P \times R \times |\dot{\delta}_{d,i}^{j-1}| - 10)}}, \\ \frac{A_{d,i,1-3}^j}{F_{d,i}^{j-1}} \leq G, \\ C_{d,i,1-3}^j > 0, \end{cases}
 \end{cases} \tag{5a}$$

$$\tag{5b}$$

where  $F_{d,i}^j$  is the damping force of the  $i$ th story at the  $j$ th time step;  $F_{d,i}^{j-1}$  is the  $i$ th story damper force at the  $(j - 1)$ th time step (i.e. the previous control time step);  $C_{d,i,2-4}^j$  and  $C_{d,i,1-3}^j$  are the damping coefficients of the  $i$ th story at the  $j$ th time step

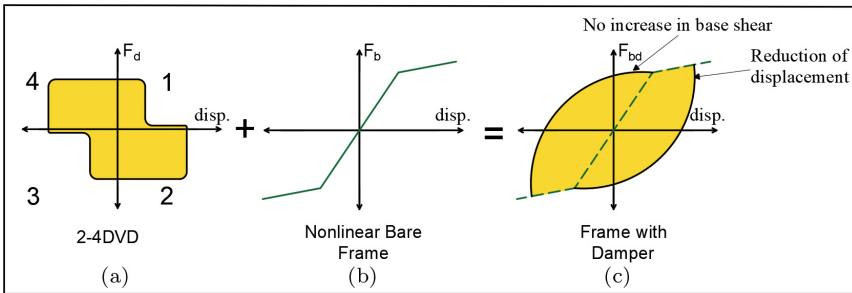


Fig. 7. Schematic representation of idealized semiactive 2-4DVD control.  $F_d$  = damper force.  $F_b$  = base shear for bare frame (without damper).  $F_{bd}$  = total base shear for damped structure.

for quadrants 2–4 and for quadrants 1–3, respectively; and  $A_{i,1-3}^j$  and  $A_{i,2-4}^j$  are time-dependent variables of the  $i$ th story at the  $j$ th time step in quadrants 1–3 and 2–4, respectively.

The working principle of the proposed algorithm is that the initial damping coefficient  $C_{d,in}$  is updated according to the ratios  $\frac{A_{i,2-4}^j}{F_{d,i}^{j-1}}$  and  $\frac{A_{i,1-3}^j}{F_{d,i}^{j-1}}$ . A minimum damping coefficient in Eq. (5b) ( $C_{d,i,1-3}^j > 0$ ) is set to prevent convergence issues in the algorithm time steps (i.e. in Eq. (5b),  $A_{i,1-3}^j$  can reach close-to-zero values for some drifts).

The identification of the algorithm parameters given in Eq. (5) should follow the order of  $C_{d,in}$ ,  $R$ ,  $K_i^{(0)}$ ,  $P$ ,  $K_i$ , and  $G$ , as follows:

**Determination of  $C_{d,in}$ :** The initial damping coefficient  $C_{d,in}$  used in the algorithm can take any value, primarily because this value is updated in the iterative design methodology of the new 2–4DVD control proposed in this study. A value of 100 kNs/m is adopted here, and such value could be used for any low-rise frame.

**Determination of  $R$ :** The parameter  $R$  in Eq. (5b) depends on the input units and should be taken in accordance with. For instance, if  $\delta_d$  is in meters, then  $R = 100$ .

**Determination of initial parameter  $K$  ( $K_i^{(0)}$ ) and parameter  $P$ :** Parameter  $K$  relates to the energy in the quadrants. An initial  $K$  ( $K_i^{(0)}$ ) value at  $i$ th story is used to initialize the first iteration of the algorithm. The following equation can be used to calculate the initial value:

$$K_{in} = C_{d,in} \times \dot{\delta}_{d,i} \times \delta_{d,i}. \tag{6}$$

The variables  $\dot{\delta}_{d,i}$  and  $\delta_{d,i}$  could have any value. In this study, values  $\dot{\delta}_{d,i} = 1$  m/s and  $\delta_{d,i} = 1$  m are adopted in the analysis, and therefore  $K_i^{(0)} = 100$  kNm, a value which could be used for any low-rise nonlinear frame as an initial value.

Parameter  $P$  controls the force length (along the displacement loop) in quadrants 1 and 3 and as such an optimum value of  $P$  needs to be defined. To achieve this, a parametric analysis is carried out by subjecting the frame with 2–4DVD control (Eq. (6)) to the CAP record considering two cases:

- (1) Assuming a constant  $K = 40 \times K_i^{(0)}$  and  $P = 4, 6$ , and 15, as shown in Fig. 8, and
- (2) Assuming a constant  $P = 6$  and  $K = 20 \times K_i^{(0)}, 40 \times K_i^{(0)}$  and  $80 \times K_i^{(0)}$ , as shown in Fig. 9.

Table 2. Parameter  $R$  as a function of the input unit.

Input unit	$R$
m	100
cm	1
mm	0.1
inch	2.54

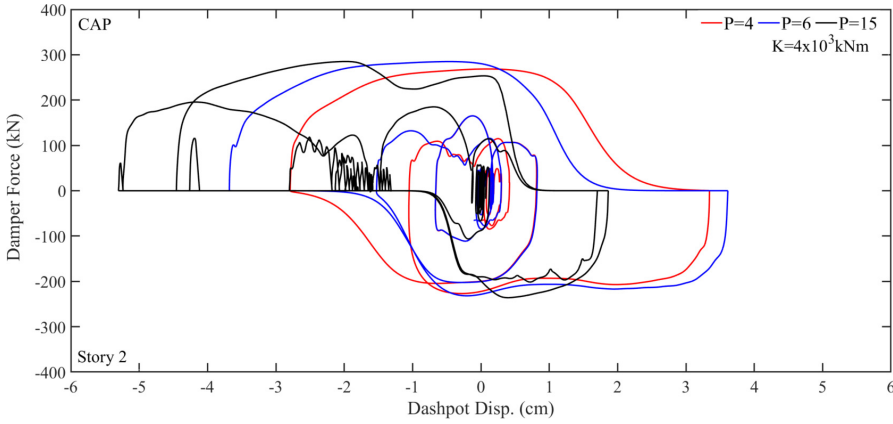


Fig. 8. Damper force vs. dashpot displacement of 2-4DVD control for constant  $K$  and different  $P$  values in story 2 (CAP record).

The values of the parameters  $C_{d,in}$ ,  $R$  and  $K_i^{(0)}$  are as defined above. Parameter  $G$  is set to be infinitely large for this parametric analysis. Note that only one record and three  $P$  values are considered here as an example. However, the selection of an optimum value  $P$  has to be carried out on an *ad hoc* basis considering different frames and different earthquake records.

Figure 8 compares 2nd story damper force vs. dashpot displacement assuming a constant  $K$  ( $4 \times 10^3$  kNm) and three different  $P$  values ( $P = 4, 6$ , and  $15$ ). All three stories have the same  $K$  and  $P$  values in the analysis. Fig. 8 shows the results for the 2nd story because this story experienced the largest inter-story drift in the frame. The results in Fig. 8 indicate that the damper forces in quadrants 1 and 3 tend to be “cut” sooner as the value of  $P$  increases (e.g. compare forces given by  $P = 15$  against

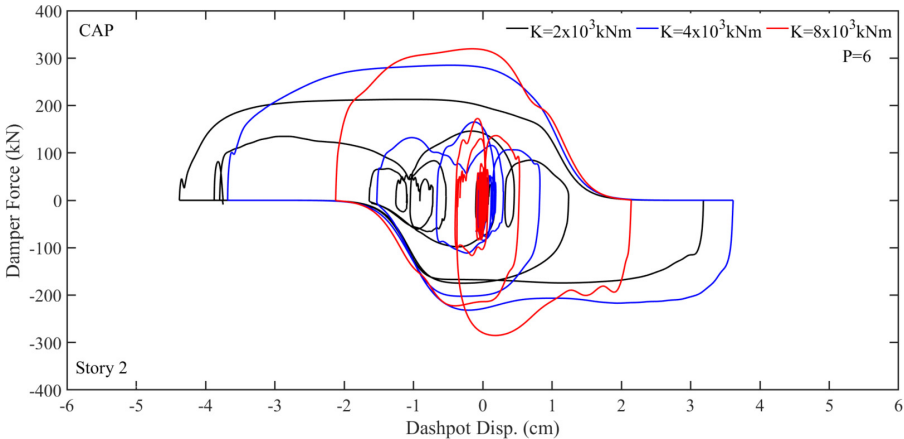


Fig. 9. Damper force vs. dashpot displacement of 2-4DVD for different  $K$  with constant  $P$  values in story 2 (CAP record).

$P = 4$ ). The results of Fig. 8 suggest that a value  $P = 6$  provides a reasonable balance between the damper force and dashpot displacement for the case study frame examined in this study.

Figure 9 compares damper force vs. dashpot displacement for a constant  $P$  ( $P = 6$ ) and three different  $K$  values ( $K = 2 \times 10^3$  kNm,  $4 \times 10^3$  kNm and  $8 \times 10^3$  kNm). All three stories have the same  $K$  and  $P$  values in the analysis. The results in Fig. 9 show that  $K = 8 \times 10^3$  kNm leads to larger damping forces than  $K = 2 \times 10^3$  kNm. The results in Fig. 9 imply that the selection of  $K$  can change significantly the shape and damper force and, as a result, such parameter needs to be optimized in the design. Based on these results, a value  $P = 6$  is adopted in subsequent analyses that aim to determine the optimum  $K_i$  of the case study frame with 2–4DVD control.

**New design methodology to determine the optimum  $K_i$ :** Figure 10 shows the flowchart of a new design methodology that can be adopted to calculate the parameter  $K_i$  at each  $i$ th story of a frame with 2–4DVD control. The frame equipped with 2–4DVD control at the  $i$ th story should be run under a critical earthquake, and  $K_i^{(0)}$  should be updated according to the iterative methodology in Fig. 10. Note that the proposed design methodology has to be applied to the  $i$ th story with a 2–4DVD control. If the same 2–4DVD control is used in more than one story, then the values  $C_{d,in}$ ,  $R$ ,  $K_i^{(0)}$  and  $P$  can be the same, but the design methodology in Fig. 10 should be applied to each story separately because the total shear force of each story is different and therefore the optimum  $K_i$  is different for each story.

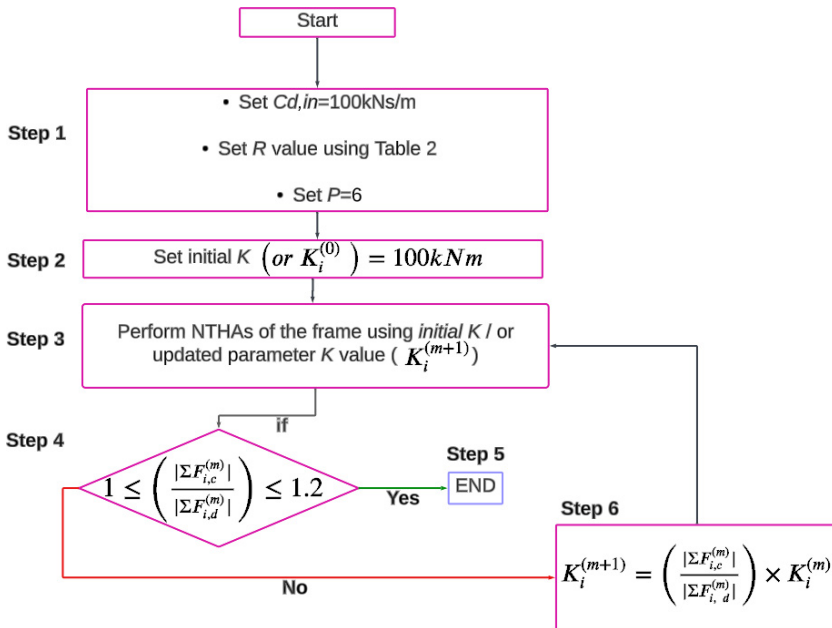


Fig. 10. Flowchart of new design methodology to define the parameter  $K_i$  in 2–4DVD control.

The new design methodology can be summarized as follows:

**Step 1.** Set the initial damping coefficient  $C_{d,in}$ , parameter  $R$  and parameter  $P$  (for the case study frame  $C_{d,in} = 100$  kNs/m,  $R$  was taken from Table 2, and  $P = 6$ ).

**Step 2.** Set the initial value of parameter  $K_i^{(0)}$  (for the case study frame  $K_i^{(0)} = 100$  kNm).

**Step 3.** Perform a NTHA of the frame using initial  $K_i^{(0)}$  or updated  $K_i$  ( $K_i^{(m+1)}$ ) value under a critical earthquake.

**Step 4.** Check if the condition in Eq. (7) is met:

$$1.0 \left( \frac{\left| \sum F_{i,c}^{(m)} \right|}{\left| \sum F_{i,d}^{(m)} \right|} \right) \leq 1.2, \tag{7}$$

where all variables are as defined before. The limits 1.0–1.2 given in Eq. (7) are provisionally suggested as lower and upper boundaries for the control proposed in this study. Note that the limits of 1 and 1.2 in Eq. (5) are set based on results from this study and could be slightly different for other case study structures.

**Step 5.** If the condition in Eq. (7) is met, then finish simulation.

**Step 6.** If the condition in Eq. (7) is not met, then update the value of parameter  $K_i^{(m)}$  based on the total global forces in columns and dampers using the recurrence relation in Eq. (8). After the update, repeat the process (from Step 3) until the condition in Eq. (7) is met.

$$K_i^{(m+1)} = \left( \frac{\left| \sum F_{i,c}^{(m)} \right|}{\left| \sum F_{i,d}^{(m)} \right|} \right) \times K_i^{(m)}, \tag{8}$$

where some variables are as defined before.  $K_i^{(m)}$  and  $K_i^{(m+1)}$  in Eq. (8) refer to  $i$ th story current and updated parameter  $K_i$  value, respectively.

**Determination of  $G$  for the case study steel frame:** Once the optimum  $K_i$  is defined, the parameter  $G$  should be calculated. To achieve this, the ratio  $\frac{A_{i,2-4}^j}{F_{d,i}^{j-1}}$  or  $\frac{A_{i,1-3}^j}{F_{d,i}^{j-1}}$  should be smaller than a given value  $G$  in order to impose a limit to the maximum value of damping coefficient.  $G$  has to be limited as otherwise the damping coefficients calculated by the proposed methodology could reach large values impossible to be achieved in practice. Therefore, the maximum value of  $C_d$  should be limited without changing the results of the optimum control achieved by using the proposed methodology. The value of  $G$  can be easily found after a couple of simulations. For instance, after identifying the optimal  $K_i$ , a first NTHA of the frame with 2–4DVD control under the selected earthquake should be performed with an infinite large  $G$  (i.e. removing the maximum limit in  $\frac{A_{i,1-3}^j}{F_{d,i}^{j-1}}$  and  $\frac{A_{i,2-4}^j}{F_{d,i}^{j-1}}$ ). This frame should be run a



second time with the same 2-4DVD control under the same ground motion as the first NTHA but with a limit on  $G$  (e.g. 300, 400, etc.). If the results (e.g. inter-story drift) from both analyses are the same, then the correct value of parameter  $G$  is found. If these two results are different ( $>1\%$ ) from each other, then increase the value of  $G$  and repeat the NTHA of the frame again under the same conditions adopted in the previous simulation. The process is repeated until the results from both analyses are the same. The following section presents and discusses the most relevant results from the NTHA carried out on the three case study steel frames with 2-4DDD, NVD, and 2-4DVD damper controls.

### 3. Results and Discussion

#### 3.1. Frames subjected to CHU record

Figures 11(a)–11(c) compare the force–displacement loops of 2-4DDD, NVD, and 2-4DVD controls at story 2 for seismic record CHU, respectively. The force is the total shear force resisted by all four columns at a story level. Story 2 is examined because this floor had the largest drift during the analyses. It is shown that 2-4DDD (see Fig. 11(a)) is less stable than 2-4DVD control loop (Fig. 11(c)). Unnecessarily large fluctuations (i.e. force “jumping”) in the loops increase the required damper forces, which in turn increases the cost of dampers. As shown in Fig. 11(a), the loop fluctuations in 2-4DDD control could raise questions about its stability and effectiveness at high earthquake frequencies. The results of Figs. 11(a)–11(c) suggest that 2-4DDD control has the largest damping force (i.e. 501 kN; Fig. 11(a)) of the three controls. To obtain the results of Fig. 11(b), the damping coefficients of NVD control

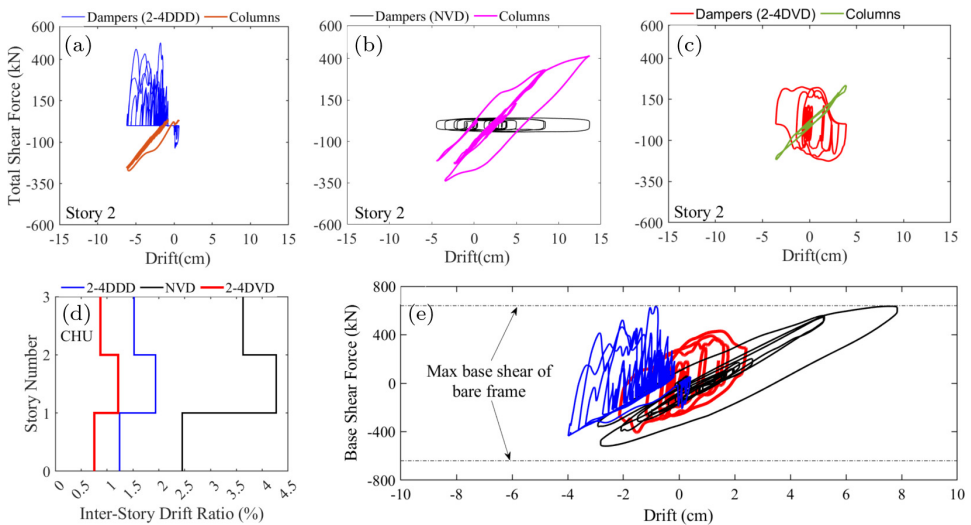


Fig. 11. NTHA results of frames with 2-4DDD, NVD, and 2-4DVD controls: (a–c) total shear force for story 2, (d) inter-story drift ratio, and (e) base shear force (CHU record).

Table 3. Main results of frames with different controls subjected to seismic records ( $\Delta$  = Reduction).

Record	Control	Max. damper force of all three stories		Max. inter-story drift of the frame (cm)		Base shear of the frame		Max. acceleration of the frame	
		(kN)	$\Delta$ (%)	(cm)	$\Delta$ (%)	(kN)	$\Delta$ (%)	(cm/s <sup>2</sup> )	$\Delta$ (%)
CHU	NVD	—	—	13.66	—	635.22	—	320	—
	2-4DDD	575.0	—	6.19	-55	635.22	0	2440.2	+662.6
	2-4DVD	231.2	-60	3.89	-72	430.46	-32	320	0
PAR	NVD	—	—	16.76	—	600.55	—	594	—
	2-4DDD	445.15	—	9.37	-44	585.46	-3	1701.6	+186.5
	2-4DVD	310.20	-30	4.89	-71	574.73	-4	396.2	-33.3
CAP	NVD	—	—	6.50	—	453.65	—	1309.8	—
	2-4DDD	324.05	—	5.33	-18	441.72	-3	1133.6	-13.5
	2-4DVD	218.59	-33	3.77	-42	423.68	-7	827.5	-36.8
KOBE	NVD	—	—	10.85	—	684.03	—	754.8	—
	2-4DDD	497.60	—	8.27	-24	647.08	-5	1631.8	+116.2
	2-4DVD	356.77	-28	5.96	-45	591.14	-14	442.5	-41.4

are distributed uniformly over all three stories of the frame and then uniformly increased until the base shear of the controlled frame reaches the maximum base shear of the bare frame. The results of Fig. 11(d) indicate that the columns of the frame with NVD control experienced a large 4.3% inter-story drift ratio. Therefore, NVD-controlled structural elements are likely to have more structural damage. The results of Fig. 11(d) showed that, compared to the NVD control, the 2-4DDD control reduced the maximum inter-story drift ratio by 55% in story 2 (see numerical results in Table 3), yet it increased the acceleration of the frame by 662.6% at story 1 (see last column of Table 3) under the same base shear force as the bare frame (dashed black lines in Fig. 11(e)). However, the 2-4DVD control is more effective than the NVD control, with a 72% reduction in inter-story drift ratio and a 32% reduction in base shear forces (see Table 3 and Fig. 11(e)). The 2-4DVD control also reduced the maximum acceleration of the bare frame by 32% (Fig. 12(c)). The large acceleration in story 1 can be attributed to the large damping forces created by 2-4DDD control. The base shear force, shown in Fig. 11(e), is obtained by summing up the global forces from the two damper forces and all four columns in story 1. The maximum base shear force of the bare frame, shown in Fig. 11(e) (without controls, as given in Fig. 2(a)), is obtained by subjecting the frame to CHU earthquake. The results (see Table 3) show that the maximum damper force required by the 2-4DVD control is 60% lower than that of the 2-4DDD control (231.2 kN vs. 575.0 kN respectively).

Past research has shown that residual deformations after a mainshock can worsen the seismic performance of frames during aftershocks (De Domenico *et al.*, 2024; Yan *et al.*, 2024). As a result, frames should be able to recenter themselves after an earthquake. Figures 12(a) and 12(c) compare, respectively, the inter-story drifts, velocities and accelerations of the bare frame and the frames with three controls (NVD, 2-4DDD, and 2-DVD) subjected to the CHU record. Figures 12(d) and 11(a) show that the largest inter-story drift occurred in story 2. If the recentering capacity

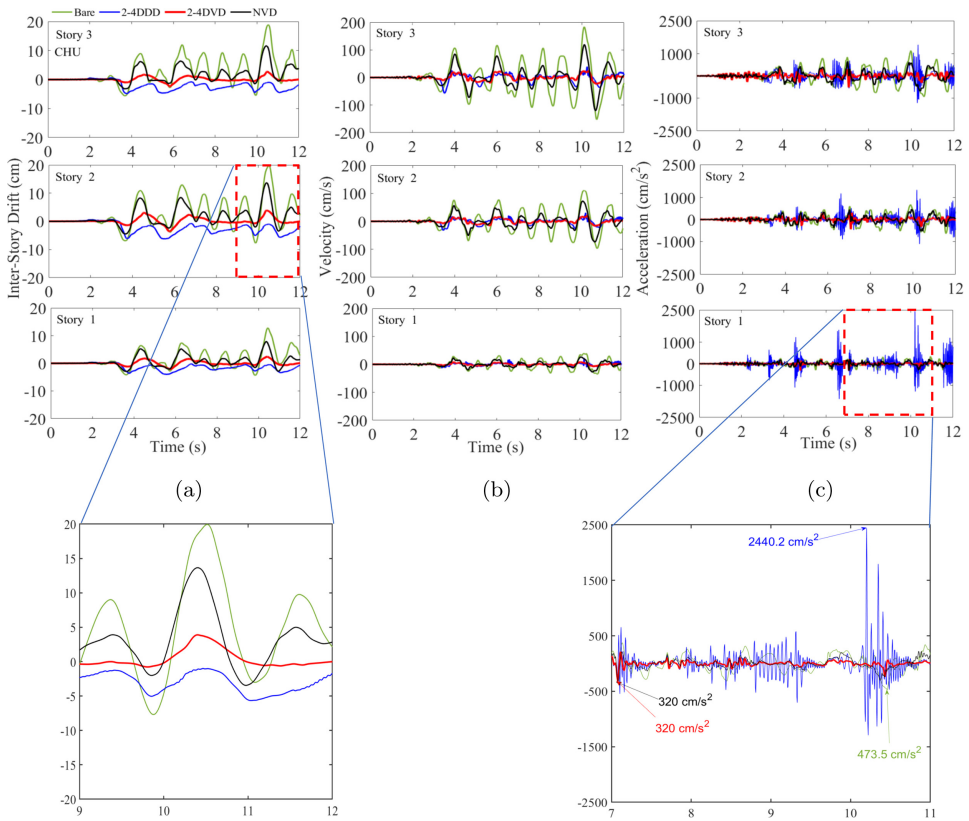


Fig. 12. NTHA results of bare frame and frames with 2-4DDD, NVD, and 2-4DVD controls: (a) inter-story drifts, (b) velocities, and (c) accelerations at stories 1, 2, and 3 (CHU record).

of the three controls is evaluated in story 2, it is noted that the residual deformation of the bare, NVD and 2-4DDD frames is not zero, whereas the 2-4DVD frame practically has zero drifts. The residual drifts in the bare, NVD and 2-4DDD frames can be attributed to the nonlinear behavior in beams and columns. This is confirmed by the widespread plastic hinging experienced by such frames under the CHU record, as shown in Fig. 13. Conversely, the frame with 2-4DVD control remains essentially linear under the same earthquake. Figure 13 also indicates that the maximum joint rotation  $\theta_{\max}^b$  of beams in the frame with 2-4DDD control is 0.015 radians, whereas this value is only 0.01 rad in the frame with 2-4DVD control. Overall, the reduced damper force fluctuations in the hysteresis loops (due to large fluctuations in velocity, as shown in Fig. 12(b)) achieved by the 2-4DVD control improved the frame's seismic performance under the CHU record. On the other hand, the sudden fluctuations in the damper force of the 2-4DDD control easily increase the base shear of the frame. This limits the use of such control since the design objective of this study is to reduce the inter-story drift but without increasing the base shear of the frame.

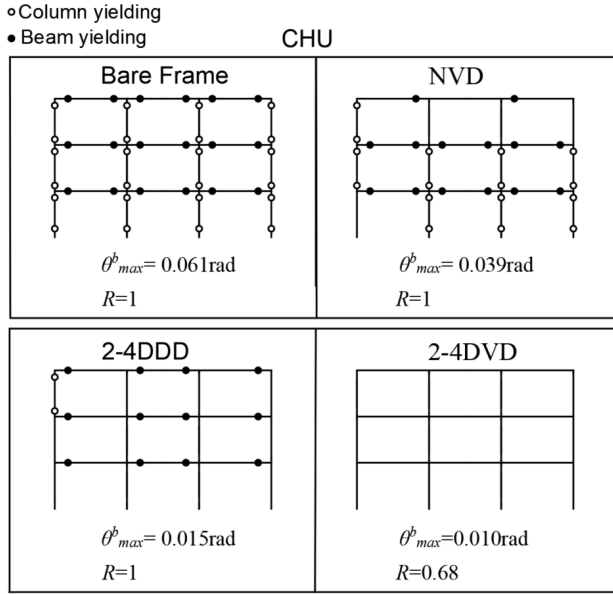


Fig. 13. Plastic hinging in frames with different controls (CHU record).  $\theta_{max}^b$  = maximum rotation at beam-column joints.  $R$  = ratio of base shear of controlled frames (NVD, 2-4DDD, or 2-4DVD) to the base shear of bare frame.

Figure 14(a) compares the base shear force of the bare frame and that of the frames with the three control systems. The results in Fig. 14(a) show that 2-4DVD control reduced the base shear due to having a more stable damper force in the quadrants. However, this generally resulted in a lower energy dissipation capacity when compared to the 2-4DDD control, as demonstrated in Fig. 14(b).

### 3.2. Frames subjected to PAR record

Figures 15(a)–15(c) compare, respectively, the force–displacement loops of 2-4DDD (at story 3), NVD (story 3), and 2-4DVD (story 2) controls at the largest inter-story drift ratio for seismic record PAR. The force–displacement loop in other stories can also be compared, but this study considered the story where the maximum inter-story drift occurs. A comparison between the hysteresis loops of 2-4DDD (Fig. 15(a)) and 2-4DVD controls (Fig. 15(c)) indicates that 2-4DDD is less stable. Figure 15(d) illustrates the maximum inter-story drift ratio of the frame for different controls. Similar to the CHU record, story 3 of the frame with NVD control experienced a large maximum drift ratio of 5.2%, as shown in Fig. 15(d). Figure 15(e) illustrates the total base shear force vs. drift of story 1 for three different controls. The results show that, compared to NVD control, 2-4DDD control reduced the inter-story drift ratio by 44% (Fig. 15(d) and Table 3), the total base shear force by 2.5% (Fig. 15(e) and Table 3), yet increased the acceleration of the frame by 186.5% at story 1 (see Table 3) under the same base shear force as the bare frame (dashed black lines in

A. Kiral et al.

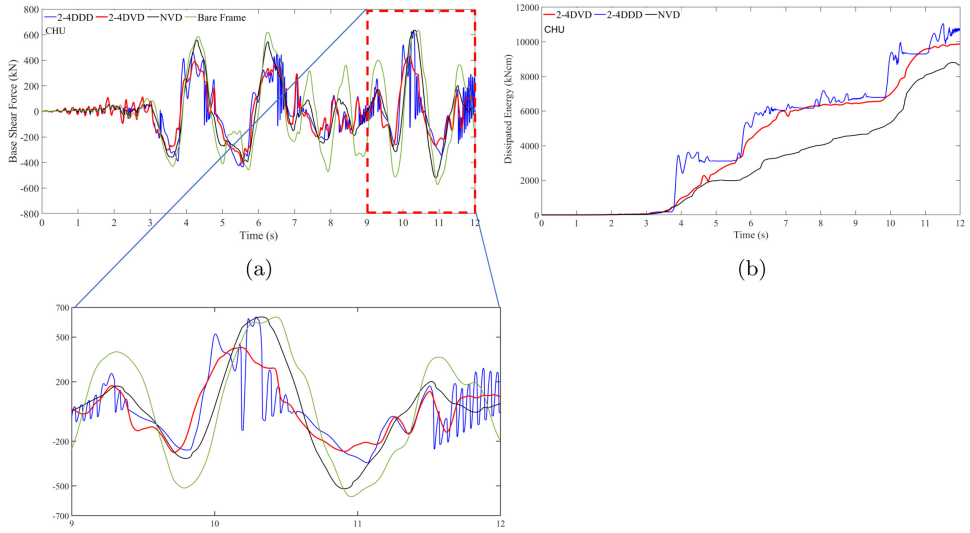


Fig. 14. NTHA results of bare frame and frames with 2-4DDD, NVD, and 2-4DVD controls: (a) time history of base shear, (b) time history of total dissipated energy by the dampers (CHU record).

Fig. 11(e)). The reason for the large acceleration in story 1 is the large damping forces generated by 2-4DDD control. 2-4DVD control outperformed NVD control and reduced the maximum inter-story drift ratio by 71% (Fig. 15(d) and Table 3), and the total base shear force by 4.3% (Fig. 15(e) and Table 3). 2-4DVD also reduced the maximum acceleration of the bare frame by 29% (see Fig. 16(c)). The results in

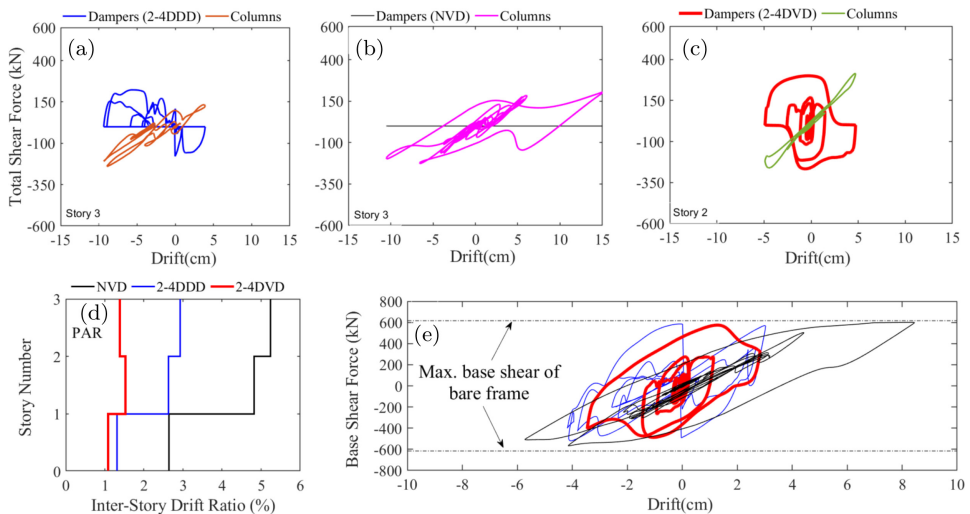


Fig. 15. NTHA results of frames with 2-4DDD, NVD, and 2-4DVD controls: (a, b, and c) total shear force of stories 3, 3, and 2, respectively, (d) inter-story drift ratio, and (e) total base shear force (PAR record).

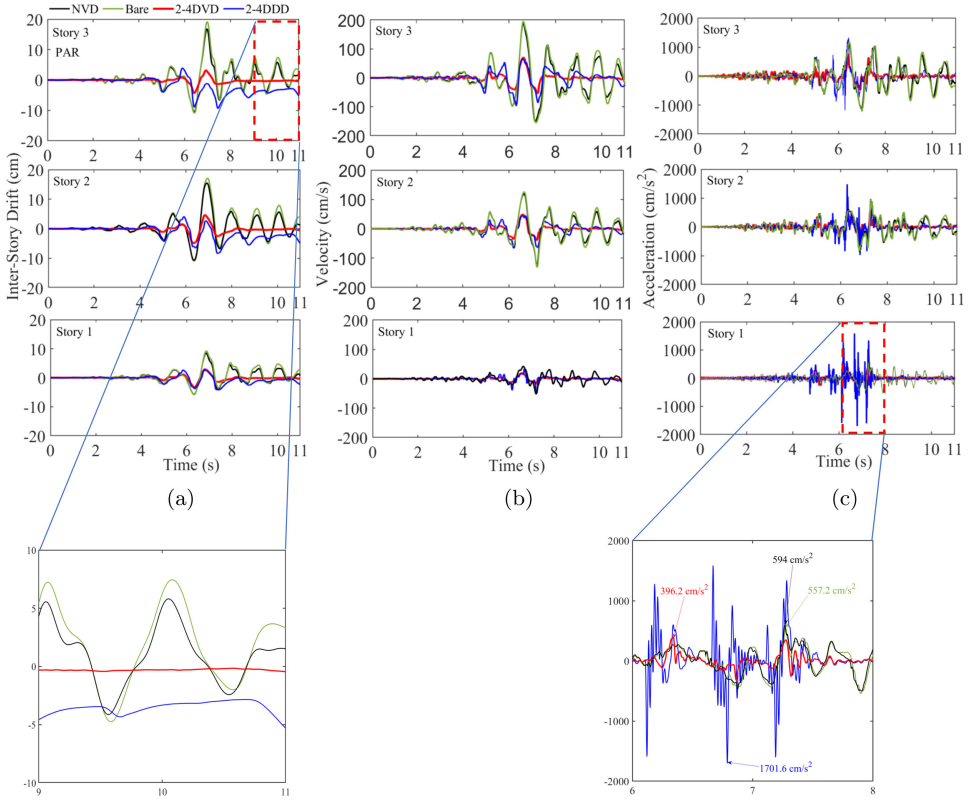


Fig. 16. NTHA results of bare frame and frames with 2-4DDD, NVD, and 2-4DVD controls: (a) inter-story drifts, (b) velocities, and (c) accelerations at stories 1, 2, and 3 (PAR record).

Table 3 indicate that 2-4DVD control requires 30% less maximum damper force than 2-4DDD control.

Figures 16(a) and 16(c) compare, respectively, the inter-story drifts, velocities, and accelerations of the bare frame and the frames with three controls (NVD, 2-4DDD, and 2-DVD) subjected to the PAR record. The results in Figs. 16(d) and 15(a) show that the third story has the largest inter-story drift if NVD and 2-4DDD controls are used. If the controls' recentering capacities are considered in story 3, the residual deformation of the bare frame and frames with NVD and 2-4DDD controls is not zero, whereas the frame with 2-4DVD controls almost achieved zero drifts. This is because the beams and columns of the bare frame and the frames with NVD and 2-4DDD controls exhibited highly nonlinear behavior, whereas 2-4DVD experienced comparatively less yielding in the frame (see Fig. 17). The maximum joint rotation  $\theta_{max}^b$  of the beams in the frame with 2-4DDD control is 0.026 rad, whereas such value is only 0.012 rad in the frame with 2-4DVD control. Overall, the seismic performance of the frame under the PAR record was enhanced by the decreased damper force fluctuations (i.e. velocity; as seen in Fig. 16(b) in the

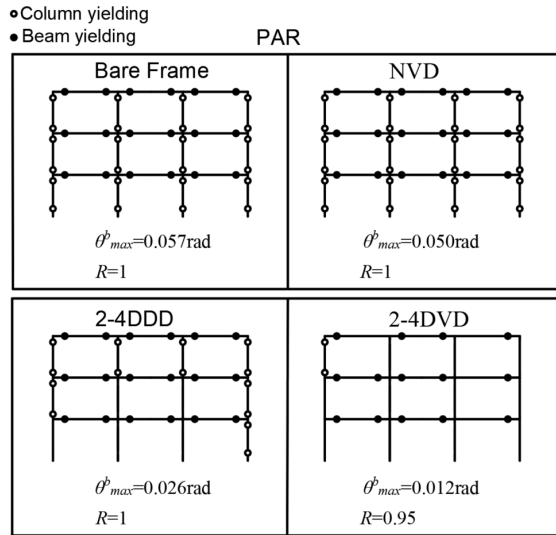


Fig. 17. Plastic hinging in frames with different controls (PAR record).  $\theta_{max}^b$  = maximum rotation at beam-column joints.  $R$  = ratio of base shear of controlled frames (NVD, 2–4DDD, or 2–4DVD) to the base shear of bare frame.

hysteresis loops, which is achieved by 2–4DVD control. Sudden variations in the damper force of the 2–4DDD control system can significantly increase the base shear of the frame structure. Consequently, these abrupt changes restrict the use of such controls in nonlinear MDOF systems.

Figures 18(a) compares the base shear force of the bare frame and that of the frames with the three control systems. The results show that whilst the 2–4DVD control generally resulted in smaller energy dissipation than the 2–4DDD control (the largest drift occurs between 6 s and 8 s; see Fig. 18(b)), it slightly reduced the base shear due to its more stable damper force in the quadrants. As mentioned in Secs. 2.4 and 2.5, the rationale behind using the controls (2–4DDD or 2–4DVD) is to minimize inter-story drift without increasing the base shear of the frame. By allowing some forces in quadrants 1 and 3, the proposed control algorithm improves the frame behavior compared to the 2–4DDD control.

### 3.3. Frames subjected to CAP record

For seismic record CAP, Figs. 19(a)–19(c) compares the force–displacement loops of 2–4DDD, NVD, and 2–4DVD controls at the story in which the maximum inter-story drift occurs, stories 3, 2, and 2, respectively. The hysteresis loop of 2–4DDD is less stable (Fig. 19(a)) than 2–4DVD control loop (Fig. 19(c)). Comparing 2–4DDD control to NVD, it is shown that 2–4DDD control reduced the inter-story drift ratio by 18% (Fig. 19(d) and Table 3), the base shear force by 2.6% (Fig. 19(e) and Table 3), and the acceleration of the frame by 13.5% (see Table 3) under the same base shear force as the bare frame (dashed black lines in Fig. 19(e)). The results in

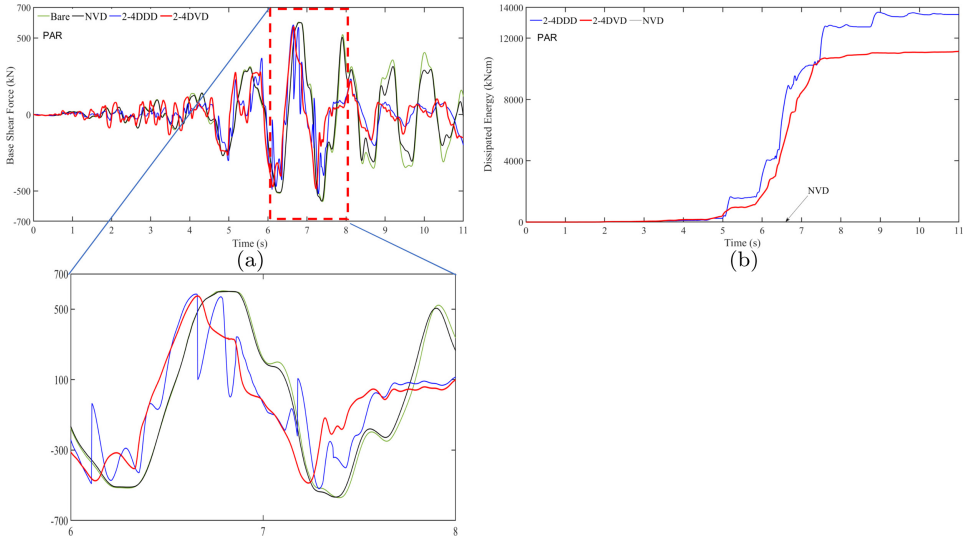


Fig. 18. NTHA results of bare frame and frames with 2-4DDD, NVD, and 2-4DVD controls: (a) time history of base shear, (b) time history of total dissipated energy by the dampers (PAR record).

Table 3 show that 2-4DVD control requires 32.5% less maximum damper force than 2-4DDD control. Moreover, 2-4DVD control outperforms NVD control by reducing the inter-story drift ratio by 42% (Fig. 19(d)) and shear force by 6.6% (Fig. 19(e) and Table 3]. 2-4DVD also reduced the maximum acceleration of the bare frame by 42% (see Fig. 20(c)). The results in Table 3 indicate that the 2-4DVD control requires 33% less maximum damper force than the 2-4DDD control.

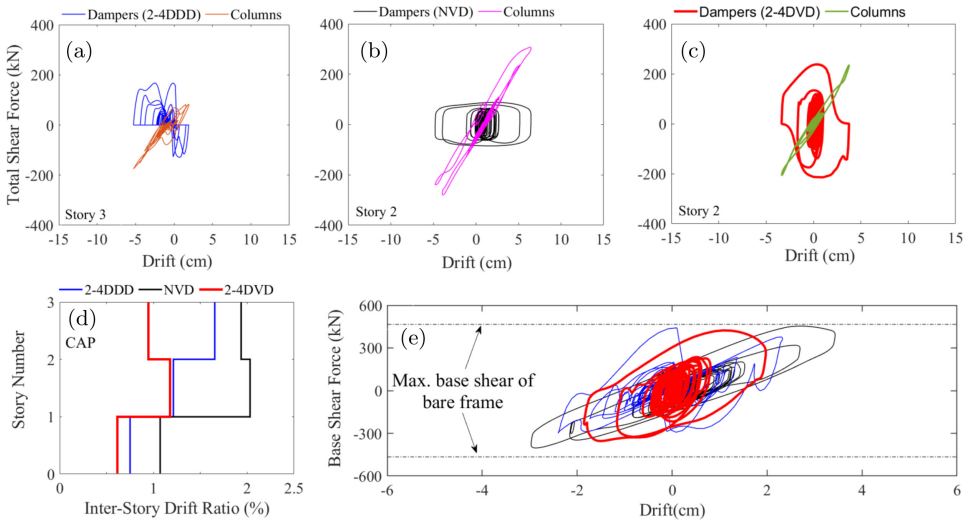


Fig. 19. NTHA results of frames with 2-4DDD, NVD, and 2-4DVD controls: (a-c) total shear force of stories 3, 2, and 2, respectively, (d) inter-story drift ratio, and (e) total base shear force (CAP record).



A. Kiral et al.

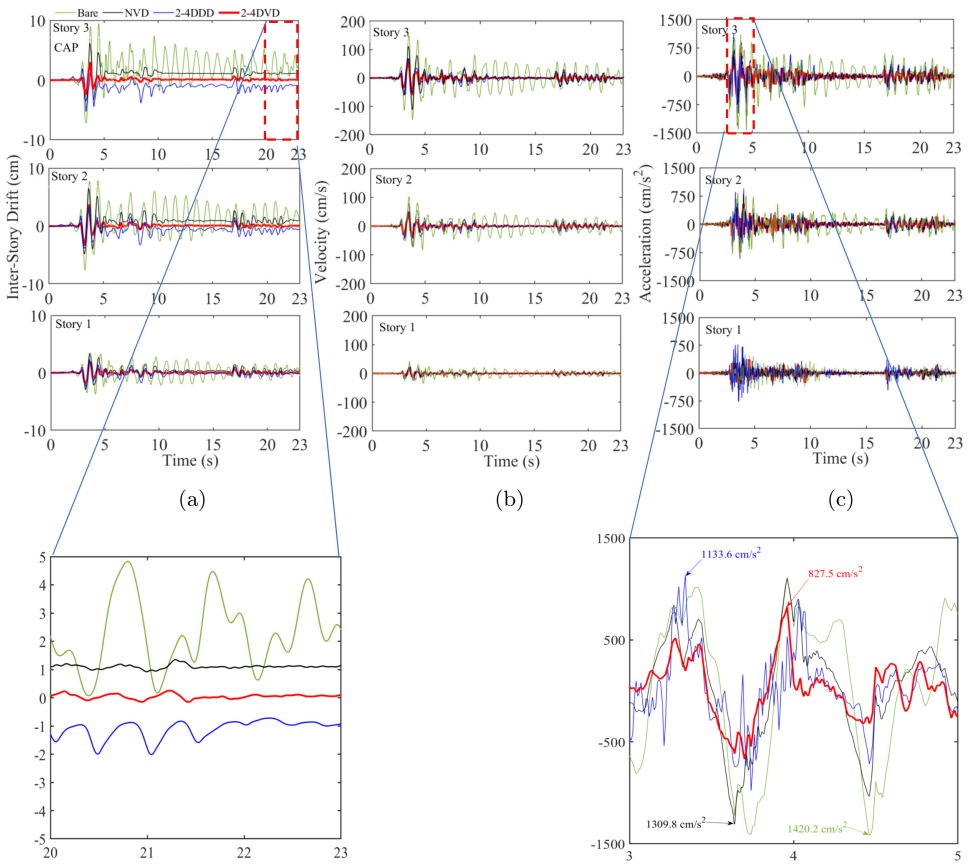


Fig. 20. NTHA results of bare frame and frames with 2-4DDD, NVD, and 2-4DVD controls: (a) inter-story drifts, (b) velocities, and (c) accelerations at stories 1, 2, and 3 (CAP record).

Figures 20(a) and 20(c) compare, respectively, the inter-story drifts, velocities, and accelerations of the bare frame and the frames with three controls (NVD, 2-4DDD, and 2-4DVD) subjected to the CAP record. The residual deformation of bare, NVD, and 2-4DDD is not zero when the three controls' recentering capabilities are evaluated at story 3 (story with more widespread yielding). Conversely, the frame with the 2-4DVD control nearly reached zero drift. This is because, as shown in Fig. 21, the beams and columns of the frame with 2-4DVD control remained linear. The beam's maximum rotation  $\theta_{\max}^b$  in 2-4DDD is 0.014 rad, versus 0.010 rad in the frame with 2-4DVD control. The reduced damper force fluctuations (i.e. velocity; as shown in Fig. 20(b)) in the hysteresis loop, which are accomplished by 2-4DVD control, significantly improved the seismic performance of the frame under the CAP record. 2-4DDD control can cause a considerable increase in the base shear of the frame structure when the damper force is abruptly changed. Thus, the use of such controllers in nonlinear MDOF systems is questionable.

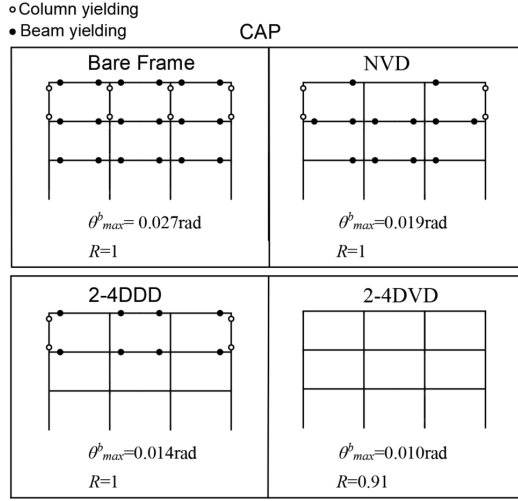


Fig. 21. Plastic hinging in frames with different controls (CAP record).  $\theta_{max}^b$  = maximum rotation at beam-column joints.  $R$  = ratio of base shear of controlled frames (NVD, 2-4DDD, or 2-4DVD) to the base shear of bare frame.

Figure 22(a) compares the base shear force of the bare frame and the frames with three control systems. From Fig. 22(a), it can be seen that the base shear force of the 2-4DVD control is smoother than that of the 2-4DDD control due to the more consistent damper forces in the quadrants. In addition, the frame with 2-4DVD control resulted in slightly reduced base shear than 2-4DDD, and in slightly higher energy dissipation (the highest drift happens between 3 s and 5 s; see Fig. 22(b)).

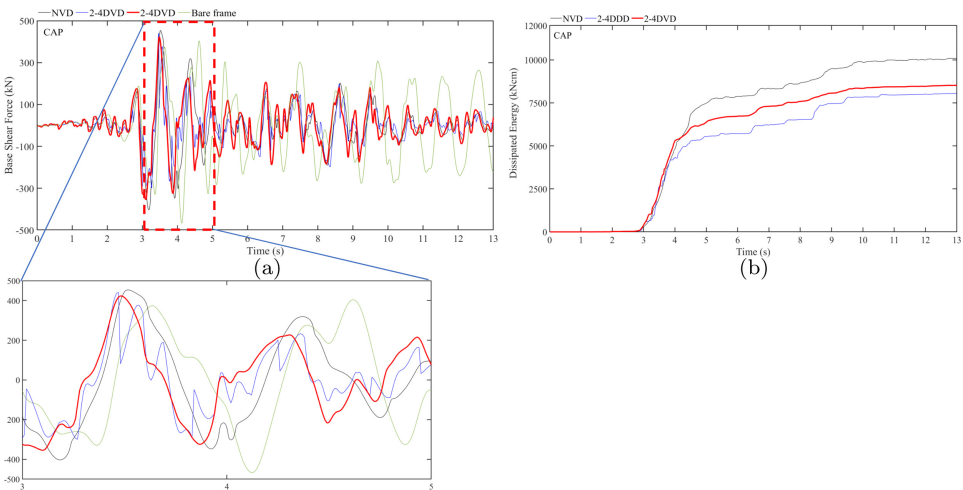


Fig. 22. NTHA results of bare frame and frames with 2-4DDD, NVD, and 2-4DVD controls: (a) time history of base shear, (b) time history of total dissipated energy by the dampers (CAP record).

### 3.4. Frames subjected to KOBE record

Figures 23(a)–23(c) compare the force–displacement loops of 2–4DDD, NVD, and 2–4DVD controls at story 2 (where the maximum inter-story drift occurs) for seismic record KOBE. Comparing 2–4DDD control to NVD, it is shown that 2–4DDD control reduced the inter-story drift ratio by 24% (Fig. 23(d) and Table 3) and the base shear force by 5.4% (Fig. 23(e) and Table 3), yet it increased the acceleration of the frame by 116.2% at story 1 (see Table 3) under the same base shear force as the bare frame (dashed black lines in Fig. 23(e)). The reason for large acceleration in story 1 is the large damping forces generated by 2–4DDD control. The results in Table 3 show that 2–4DVD control requires 28% less maximum damper force than 2–4DDD control. Moreover, 2–4DVD control outperforms NVD control by reducing the inter-story drift ratio by 45% (Fig. 23(d)) and shear force by 13.6% (Fig. 23(e) and Table 3). The use of a 2–4DVD control also reduced the maximum acceleration of the bare frame by 64% (see Fig. 24(c)).

The inter-story drift, acceleration, and velocity of the frame with three control systems (NVD, 2–4DDD, and 2–DVD) and the bare frame are displayed in Figs. 24(a)–24(c). The capacity of the frames to recenter themselves after an earthquake is crucial, as previously stated. The residual deformation of the bare frame and the frames with three control systems is not zero when the three controls’ recentering capacities are evaluated in story 2 (i.e. the story with the largest yielding). However, the frame with 2–4DVD control comparatively achieved less residual deformation than the other three frames (refer to Fig. 24(a)). Nonlinear behavior was observed in the beams and columns of the bare frame and frames with NVD, and 2–4DDD controls, but only in the beams of the frame with 2–4DVD control

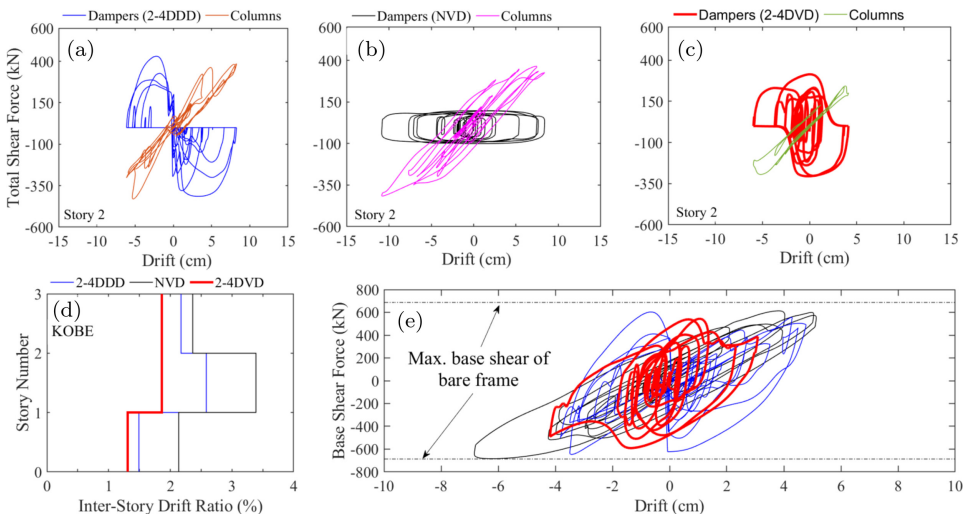


Fig. 23. NTHA results of frames with 2–4DDD, NVD, and 2–4DVD controls: (a–c) total shear force of story 2, respectively, (d) inter-story drift ratio, and (e) total base shear force (KOBE record).

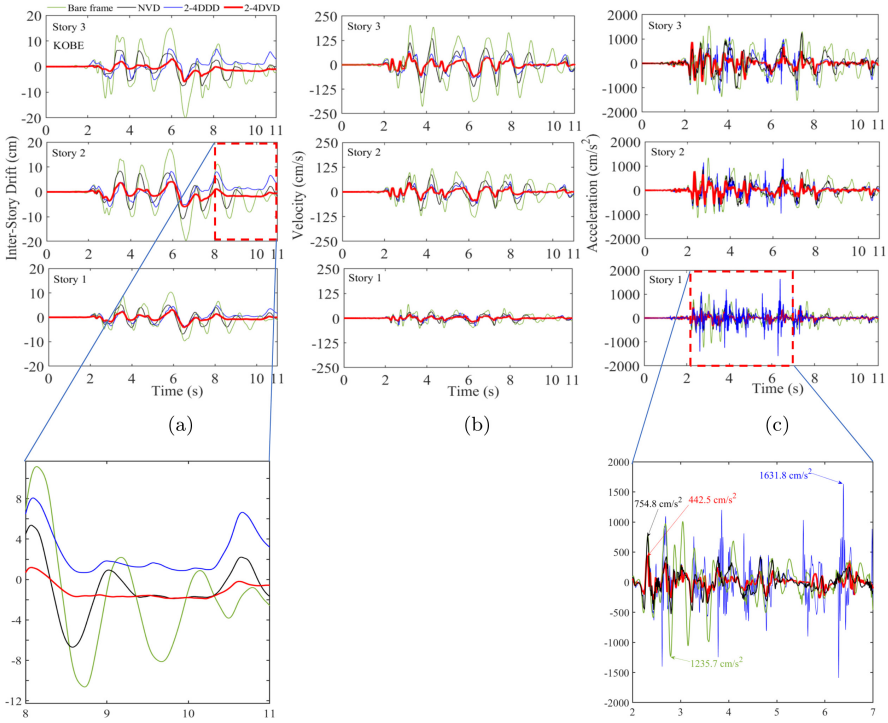


Fig. 24. NTHA results of bare frame and the frames with 2-4DDD, NVD, and 2-4DVD controls: (a) the inter-story drift, (b) velocity, and (c) acceleration at stories 1, 2, and 3 (KOBE record).

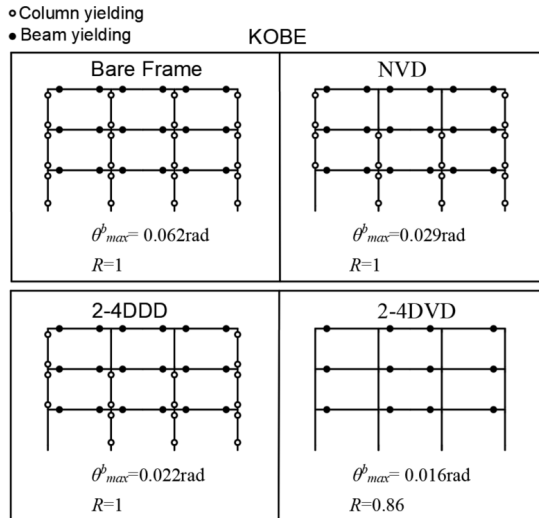


Fig. 25. Plastic hinging in frames with different controls (KOBE record).  $\theta_{max}^b$  = maximum rotation at beam-column joints.  $R$  = ratio of base shear of controlled frames (NVD, 2-4DDD, or 2-4DVD) to the base shear of bare frame.

A. Kiral et al.

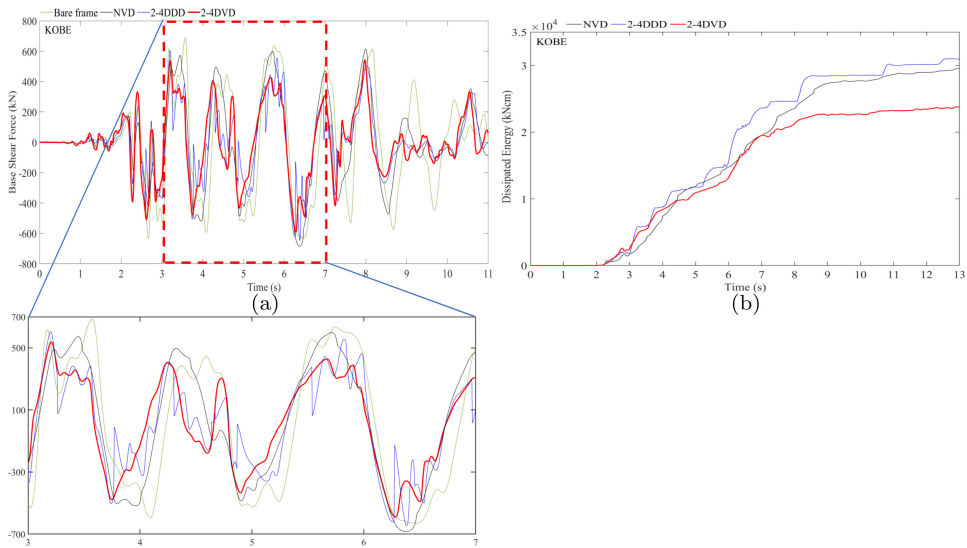


Fig. 26. NTHA results of bare frame and frames with 2-4DDD, NVD, and 2-4DVD controls: (a) time history of base shear, (b) time history of total dissipated energy by the dampers (KOBE record).

(see Fig. 25). The maximum rotation  $\theta_{\max}^b$  of the beams in the frames with 2-4DDD and 2-4DVD controls is 0.022 rad and 0.016 rad, respectively. Overall, the 2-4DVD control reduces the damper force fluctuations (i.e. see velocity in Fig. 24(b)) in the hysteresis loop, which improves the seismic performance of the frame under the KOBE record.

The base shear force of the bare frame and frame with three control systems is shown in Fig. 26(a). With a more steady damper force in the quadrants, 2-4DVD control is seen to reduce the base shear (see Fig. 25;  $R = 0.86$ ), even if it results in smaller energy dissipation than 2-4DDD (the largest drift occurs between 3 s and 7 s; see Fig. 26(b)).

The results in previous sections show that, for the four strong seismic records used in the analysis, all the drifts in the frame with NVD control are well above the other two controls (2-4DDD and 2-4DVD). It also cannot recenter itself after applying the seismic records. This implies that, if capacity design principles are followed, the use of NVD dampers in the nonlinear frame would require retrofitting the foundations and columns for high-added damping applications. The frame with 2-4DDD control performed better than the frame with NVD control by reducing frame drifts between 18% and 55% and the base shear between 0% and 5.4%. However, 2-4DDD control was proved to be unstable under the CHU record because the response wave in higher modes interferes with the response wave of the fundamental mode, leading to high-frequency oscillations in the hysteresis loop for nonlinear steel frames. Compared to the NVD control, the 2-4DDD control increased the maximum acceleration of the frame by 116.2–662.6%. If the recentering capacity of the frame with 2-4DDD control is considered, it is evident that the residual deformation of the control is not

zero under the four earthquake records due to the nonlinear behavior of the frames. The results in this paper demonstrate that 2–4DVD control offers superior performance to both NVD and 2–4DDD control under the different records by reducing inter-story drift by up to 72% in comparison to NVD control and reducing the required maximum damper force by up to 60% in comparison to 2–4DDD control. 2–4DVD control reduced the total base shear force by 4–32% (compared with NVD) for the four seismic records examined in this study. In comparison with the NVD control, the new 2–4DVD control reduced the maximum acceleration by 33.3–41.4%. Based on the evaluation of the recentering capacity of the frame with the 2–4DVD control, it was found that the residual deformation was practically zero under the four earthquake records in this study.

Overall, the results in this study confirm that 2–4DVD control is very effective at reducing inter-story drifts, acceleration, and base shear forces of the steel frames, as well as being able to recenter itself. It should be mentioned that in this paper, the 2–4DVD control was investigated using only a 3-story nonlinear steel frame subjected to four seismic records. Future research should investigate the behavior of medium- and high-rise frames with 2–4DVD control dampers subjected to different earthquakes, as well as the corresponding parameter  $P$  values for each story and the lower and upper boundary given in Step 4 of the proposed design methodology (Fig. 10). Future studies should also investigate a more general design methodology for medium- and high-rise nonlinear frames. It should be noted that this study only adopted a uniform damping coefficient distribution. As such, further research should investigate the use of alternative damping coefficient distributions. For instance, the concept of UDD by [Domenico and Hajirasouliha \(2021\)](#) could be adopted. Fully out of phase with frame forces control is also needed to calibrate numerical models and validate the results presented in this paper.

#### 4. Conclusions

This paper investigates numerically the seismic performance of MDOF systems with three different control systems. A nonlinear 3-story steel frame is modeled in OpenSees software and subjected to a set of four real PEER seismic records. The frame is modeled considering three controls: (i) passive NVDs, (ii) SA 2–4DDD dampers, and (iii) a new SA 2–4DVD damper proposed in this study. Parametric studies are conducted to determine the optimal parameters of 2–4DVD control in the frames. New design methodologies for MDOF systems with 2–4DVD and 2–4DDD controls are also proposed. Based on the findings of this research, the following conclusions can be drawn:

- For the 3-story frame examined in this study, the use of NVDs results in large drifts. Moreover, even a small uniform damping coefficient distribution of NVD in a nonlinear frame increases base shear. Therefore, NVD controls may not be a good choice for seismic retrofit of existing steel frames without increasing base shear.


- Compared to NVD control, 2–4DDD control reduced the inter-story drift ratio of the studied frame by 18–55% and base shear by 0–5%, yet it increased the maximum acceleration of the frame by 116.2–662.6%. The 2–4DDD control also resulted in non-zero residual deformation under the four earthquake records due to the nonlinear behavior of the frame. The 2–4DDD damper also proves unstable under high-frequency seismic records, which in turn unnecessarily increases the required damping forces and base shear force. Therefore, 2–4DDD control is not recommended in high-added damping applications of MDOF systems under high-frequency records.
- 2–4DVD control proposed in this study was very effective at controlling the frame behavior. It reduced inter-story drift by 42–72% compared with NVD control, and by 28–48% compared with 2–4DDD. 2–4DVD control also reduced base shear force by 4–32% compared to NVD control, and 2–32% compared with 2–4DDD control. The 2–4DVD control reduced the maximum acceleration of the frame by 33.3–41.4% over the NVD control. The residual deformation of the frame with 2–4DVD control was practically zero for the four earthquake records examined in the study.
- The maximum damper force required by 2–4DVD is another advantage over 2–4DDD since the damper force is 28–60% lower than the former. The 2–4DVD control also has more stable hysteresis loops under the seismic records used in the analysis.


It should also be noted that this study considered an ideal device control law with no delays in response. However, computation delays and the valve actuation speed can affect the overall performance of a SA device and these variables modify the results. A solution to potential time delays in control is to achieve the proposed SA control (2–4DVD) mechanically. The force–displacement hysteretic loop of such dampers can be reshaped by either a decentralized SA control [Fukuda and Kurino, 2019; Hazaveh et al., 2017b; Kurino et al., 2003] or mechanically by a passive damper [Hazaveh et al., 2017a; Nie et al., 2018]. For instance, Hazaveh et al. [2017a] introduced the development and characterization of a passive Direction and Displacement-Dependent (DDD) viscous damping device. The passive 2–4DDD viscous device by Hazaveh et al. [2017a] could be extended to obtain 2–4DVD viscous devices as well. The passively achieved 2–4DDD damper could be modified in the future by changing the oil inside, mechanically changing the hole within, or any other modifications necessary to overcome its instability in nonlinear MDOF. Moreover, this study only considered a low-rise frame and only four earthquake records due to the unstable behavior of the 2–4DDD control. As such, further research should examine the behavior of medium- and high-rise frames with a 2–4DVD control subjected to a wide range of earthquake frequencies. Further investigations should also propose general convergence criteria (given in Eqs. [3] and [7]) for low-, medium- and high-rise frames as the results are expected to be different for such buildings.


## Acknowledgments


The first author acknowledges that this research was only made possible by a fully supported PhD scholarship (2018–2022; Turkish law no. 1416) provided by the Ministry of National Education of Türkiye (Turkey).

## ORCID

Adnan Kiral  <https://orcid.org/0000-0002-4534-3686>

Reyes Garcia  <https://orcid.org/0000-0002-6363-8859>

Mihail Petkovski  <https://orcid.org/0000-0002-3788-0772>

Iman Hajirasouliha  <https://orcid.org/0000-0003-2597-8200>

## References

- Abdulahadi, M., Xun'an, Z., Fan, B. and Moman, M. [2020a] "Design, optimization and non-linear response control analysis of the mega sub-controlled structural system (MSCSS) under earthquake action," *J. Earthq. Tsunami* **14**(3), 1–25.
- Abdulahadi, M., Xun'an, Z., Fan, B. and Moman, M. [2020b] "Evaluation of seismic fragility analysis of the mega sub-controlled structural system (MSCSS)," *J. Earthq. Tsunami* **14**(6), 1–19.
- Akcelyan, S., Lignos, D. G., Hikino, T. and Nakashima, M. [2016] "Evaluation of simplified and state-of-the-art analysis procedures for steel frame buildings equipped with supplemental damping devices based on e-defense full-scale shake table tests," *J. Struct. Eng.* **142**(6), 1–17.
- Akehashi, H. and Takewaki, I. [2019] "Optimal viscous damper placement for elastic-plastic MDOF structures under critical double impulse," *Front. Built Environ.* **5**(3), 1–17.
- Altieri, D., Tubaldi, E., De Angelis, M., Patelli, E. and Dall'Asta, A. [2018] "Reliability-based optimal design of nonlinear viscous dampers for the seismic protection of structural systems," *Bull. Earthq. Eng.* **16**(2), 963–982.
- Aydin, E., Noroozinejad Farsangi, E., Öztürk, B., Bogdanovic, A. and Dutkiewicz, M. [2019] "Improvement of building resilience by viscous dampers," in *Resilient Structures and Infrastructure*. (Springer, Singapore), pp. 105–127.
- CEN Eurocode 8 [2004] CEN (European Committee for Standardisation). "Eurocode 8: Design of structures for earthquake resistance. General rules, seismic actions and rules for buildings," EN1998-1:2004. (EN 1998-1, Brussels).
- Chan, P.-T. and Quincy, T. M. [2022] "Multi-Objective optimization of viscous damper placement for building structures subjected to ground motion," *Int. J. Struct. Stabil. Dyn.* **23**(5), 1–8.
- Chase, J. G., Mulligan, K. J., Gue, A., Alnot, T., Rodgers, G., Mander, J. B., Elliott, R., Deam, B., Cleeve, L. and Heaton, D. [2006] "Re-shaping hysteretic behaviour using semi-active resettable device dampers," *Eng. Struct.* **28**(10), 1418–1429.
- Dall'Asta, A., Tubaldi, E. and Ragni, L. [2016] "Influence of the nonlinear behavior of viscous dampers on the seismic demand hazard of building frames," *Earthq. Eng. Struct. Dyn.* **45**(1), 149–169.
- Dan, M., Ishizawa, Y., Tanaka, S., Nakahara, S., Wakayama, S. and Kohiyama, M. [2015] "Vibration characteristics change of a base-isolated building with semi-active dampers before, during, and after the 2011 Great East Japan earthquake," *Earthq. Struct.* **8**(4), 889–913.



- De Domenico, D., Gandelli, E. and Gioitta, A. [2024] “Displacement-based design procedure for the seismic retrofit of existing buildings with self-centering dissipative braces,” *Structures* **62**, 106174.
- Domenico, D. and Hajirasouliha, I. [2021] “Multi-level performance-based design optimization of steel frames with nonlinear viscous dampers,” *Bull. Earth. Eng.* **19**, 5015–5049.
- Dong, B., Sause, R. and Ricles, J. M. [2016] “Seismic response and performance of a steel MRF building with nonlinear viscous dampers under DBE and MCE,” *J. Struct. Eng.* **142**(6), 1–16.
- Etedali, S., Akbari, M. and Seifi, M. [2023] “Friction tuned mass dampers in seismic-excited high-rise buildings with SSI effects: A reliability assessment,” *J. Earthq. Tsunami* **17**(2), 2250022.
- Fukuda, R. and Kurino, H. [2019] “Highly efficient semi-active oil damper with energy recovery system,” *Jpn. Archit. Rev.* **2**(3), 238–249.
- Hazaveh, N. K., Rodgers, G. W., Chase, J. G. and Pampanin, S. [2017a] “Experimental test and validation of a direction- and displacement-dependent viscous damper,” *J. Eng. Mech.* **143**(11), 1–7.
- Hazaveh, N. K., Rodgers, G. W., Chase, J. G. and Pampanin, S. [2017b] “Reshaping structural hysteresis response with semi-active viscous damping,” *Bull. Earthq. Eng.* **15**(4), 1789–1806.
- Hazaveh, N. K., Rodgers, G. W., Pampanin, S. and Chase, J. G. [2016] “Damping reduction factors and code-based design equation for structures using semi-active viscous dampers,” *Earthq. Eng. Struct. Dyn.* **45**(15), 2533–2550.
- Ho, C., Lang, Z., Billings, S. A., Kohiyama, M. and Wakayama, S. [2018] “Nonlinear damping-based semi-active building isolation system,” *J. Sound Vib.* **424**(6), 302–317.
- Hosseini Lavassani, S. H., Ebadijalal, M., Shahrouzi, M., Gharehbaghi, V., Noroozinejad Farsangi, E. and Yang, T. Y. [2022] “Interpretation of simultaneously optimized fuzzy controller and active tuned mass damper parameters under pulse-type ground motions,” *Eng. Struct.* **261**, 114286.
- Huang, H. C. [2009] “Efficiency of the motion amplification device with viscous dampers and its application in high-rise buildings,” *Earthq. Eng. Vib.* **8**(4), 521–536.
- Jiao, Y., Li, J. and Guan, Z. [2018] “Shake table studies on viscous dampers in seismic control of a single-tower cable-stayed bridge model under near-field ground motions,” *J. Earthq. Tsunami* **12**(5), 1–21.
- Karami Mohammadi, R., Ghamari, H. and Noroozinejad Farsangi, E. [2021] “Active control of building structures under seismic load using a new uniform deformation-based control algorithm,” *Structures* **33**, 593–605.
- Kiral, A. and Gurbuz, A. [2024] “Using supplemental linear viscous dampers for experimentally verified base-isolated building: Case study,” *J. Struct. Eng. Appl. Mech.* **7**(1), 34–50.
- Kostic, S. M. and Filippou, F. C. [2012] “Section discretization of fiber beam-column elements for cyclic inelastic response,” *J. Struct. Eng.* **138**(5), 592–601.
- Kurino, H., Tagami, J., Shimizu, K. and Kobori, T. [2003] “Switching oil damper with built-in controller for structural control,” *J. Struct. Eng.* **129**(7), 895–904.
- Lin, T.-K., Hwang, J. S. and Chen, K. H. [2017] “Optimal distribution of damping coefficients for viscous dampers in buildings,” *Int. J. Struct. Stab. Dyn.* **17**(4), 1–17.
- Lin, W. H. and Chopra, A. K. [2002] “Earthquake response of elastic SDF systems with nonlinear fluid viscous dampers,” *Earthq. Eng. Struct. Dyn.* **31**(9), 1623–1642.

- MATLAB [2018] “R2018a, mathematical computing software for engineers and scientists,” The MathWorks Inc., USA, Available at: <https://www.mathworks.com> (accessed on January, 2020).
- McKenna, F., Fenves, G. and Scott, M. [2006] “Computer program openSees: Open system for earthquake engineering simulation,” Available at: <https://opensees.berkeley.edu>.
- Meigooni, F. S. and Tehranizadeh, M. [2022] “Effect of mainshock–aftershock excitations on seismic energy dissipation mechanism of RC frames,” *J. Earthq. Tsunami* **16**(5), 1–9.
- Miyamoto, H. K., Gilani, A. S. J., Wada, A. and Ariyaratana, C. [2010] “Limit states and failure mechanisms of viscous dampers and the implications for large earthquakes,” *Earthq. Eng. Struct. Dyn.* **39**(11), 1279–1297.
- Mulligan, K., Chase, J. G., Mander, J. B., Rodgers, G. W. and Elliott, R. B. [2010] “Nonlinear models and validation for resettable device design and enhanced force capacity,” *Struct. Control Health Monit.* **17**(3), 301–316.
- Nie, S., Zhuang, Y., Wang, Y. and Guo, K. [2018] “Velocity & displacement-dependent damper: A novel passive shock absorber inspired by the semi-active control,” *Mech. Syst. Signal Process.* **99**, 730–746.
- PEER Ground Motion Database. [2023] “Pacific earthquake engineering research center,” Available at: <https://ngawest2.berkeley.edu/> (accessed on January, 2023).
- Quintana, H. and Petkovski, M. [2018] “Optimum performance of structural control with friction dampers,” *Eng. Struct.* **172**, 154–162.
- Riaz, R. D., Malik, U. J., Shah, M. U., Usman, M. and Najam, F. A. [2023] “Enhancing seismic resilience of existing reinforced concrete building using non-linear viscous dampers: A comparative study,” *Actuators*, **12**(4), 1–21.
- Symans, M. and Constantinou, M. [1995] “Development and experimental study of semi-active fluid damping devices for seismic protection of structures,” Technical Report NCEER-95-0011. Buffalo, NY: National Center for Earthquake Engineering Research.
- Taylor Devices Inc. [2020] “Fluid viscous dampers general guidelines for engineers including a brief history taylor dampers,” Available at: [www.taylordevices.com](http://www.taylordevices.com).
- Yan, X., Shu, G., Rahgozar, N. and Alam, M. S. [2024] “Seismic design and performance evaluation of hybrid braced frames having buckling-restrained braces and self-centering viscous energy-dissipative braces,” *J. Constr. Steel Res.* **213**, 108359.